Title of the paper

Full: Effects of change in soil environment associated with heavy precipitation on soil greenhouse gas fluxes in a Siberian larch forest near Yakutsk

Short: Greenhouse gas flux in irrigated Taiga soil

Full names of the authors

Takahiro KOIDE[1], Hideyuki SAITO[2], Tetsuoh SHIROTA[3], Go IWAHANA[4], C. M. Larry LOPEZ[5], Trofim, C. MAXIMOV[6], Shuichi HASEGAWA[2], Ryusuke HATANO[2]

Addresses of the institutions

[1]Graduate School of Agriculture, Hokkaido University, Sapporo 060-8589

[2]Research Faculty of Agriculture, Hokkaido University, Sapporo 060-8589

[3]Faculty of Agriculture, Shinshu University, Nagano 399-4598

[4]Graduate School of Environmental Science, Hokkaido University, Sapporo 060-0810

[5]United Graduate School of Agricultural Sciences, Iwate University, Morioka 020-8550

[6]Institute for Biological Problems of Cryolithozone, Siberian Branch, Russian Academy of Science, Yakutsk 677980

Full address of the author to whom correspondence about the manuscript

Koide Takahiro

Postal address: Graduate School of Agriculture, Hokkaido University, N9 W9, Sapporo 060-8589, Japan

e-mail address: koide@chem.agr.hokudai.ac.jp

Tel: +81-11-706-2503

Fax: +81-11-706-2494

Type of contribution

Full-length paper

Division

Environment

Abstract

A future increase in heavy precipitation events is predicted in boreal regions. An irrigation experiment was conducted in Taiga forest in eastern Siberia to evaluate the effect of heavy precipitation on greenhouse gas (GHG; CO_2, CH_4, and N_2O) fluxes in the soil. The GHG fluxes on the soil surface were measured using a closed-chamber method and GHG production rates in the mineral soil were estimated using the concentration-gradient method based on Fick's law. Irrigation water (20 mm day^{-1}) was applied continuously for six days (120 mm in total; the same amount of summer precipitation in this region). Greenhouse gas production rates in the organic layer (O-layer) were defined as the difference between the GHG fluxes and the GHG production rates in the mineral soil. Carbon dioxide flux was measured both in root-intact (R_s) and trenched plots (R_{mw}). The root respiration rate (R_r) was calculated as the difference between R_s and R_{mw}. Considering root distribution in the soil, we regarded CO_2 production rate in the mineral soil as microbial respiration rate in the mineral soil (R_{mm}) and microbial respiration rate in the O-layer (R_{mo}) as the difference between R_{mw} and R_{mm}. The irrigation increased both soil temperature and moisture in the irrigated plot. The R_s, CH_4 flux, and N_2O flux during the irrigation period were higher in the irrigated plot than that in the non-irrigated plot ($P < 0.05$; mean R_s ± S.D. (mg C m^{-2} h^{-1}) were 171±20 and 109±11, mean CH_4 flux ± S.D. (μg C m^{-2} h^{-1}) were -5.4±4.1 and -14.0±6.5, and mean N_2O flux ± S.D. (μg N m^{-2} h^{-1}) were 1.6±1.6 and 0.2±1.1, respectively). Soil moisture affected positively on R_{mm} and CH_4 production rate in the O-layer, negatively on R_r, and did not affect R_{mo}, the CH_4 production rate in the mineral soil, and the N_2O production rates in both the O-layer and the mineral soil. Soil temperature had a positive effect on R_r and R_{mo}. The increment of global warming potential of the soil was mainly due to the increase in microbial respiration rates. Future change in precipitation pattern in this region would accelerate decomposition of the soil organic matter.

Key words: Fick's law, greenhouse gas, irrigation, trenching method, Siberian Taiga

INTRODUCTION

Forest in Russia contains 381 Pg of carbon (C) which accounts for 54% of the total C stock in forest in the northern hemisphere (Goodale *et al.* 2002) and has an important role as C sink. Taiga forest near Yakutsk in eastern Siberia lying on permafrost keeps the soil temperature low (Eugster *et al.* 2000), so that the decomposition rate of soil organic matter would be very slow (Rodionow *et al.* 2006). In addition, the amount of precipitation in this region is very low (Japan Meteorological Agency 2004).

The Intergovernmental Panel on Climate Change (IPCC 2007) predicts that an increase in air temperature, the amount of precipitation, and heavy precipitation events will occur in the permafrost region due to global warming caused by an increase in concentration of greenhouse gases (GHGs). In Siberia, heavy precipitation events exceeding 20 mm d^{-1} significantly increased during 1936 – 1994 (Easterling *et al*. 2000). An increase in air temperature will accelerate growth of vegetation and increase in C storage of biomass and litter (Sirotenko & Abashina 2008). On the other hand, increased soil temperature accompanied by thawing of permafrost will accelerate the decomposition rate of soil organic matter, enhancing global warming (Rodionow *et al.* 2006). It is still unknown what effects the change in precipitation pattern will have on the plant growth rate and the decomposition rate of soil organic matter in this region.

Many field studies reported that precipitation or irrigation on dry soil increased the rate of soil respiration owing to an increase in soil moisture (e.g. Millard *et al.* 2008). Oberbauer *et al*. (1992) reported that precipitation events that raised the water table were found to strongly reduce soil respiration in permafrost region in Alaska. However, very few studies tried to divide the effect of precipitation on soil respiration into microbial respiration and root respiration, which are the components of soil respiration

(Bond-Lamberty *et al.* 2004). Dividing soil respiration is important to evaluate the effect of heavy precipitation on plant physiology and decomposition rate of soil organic matter. Previous studies observed large increases in root and microbial respiration due to adding water to dry soil (e.g. Borken *et al*. 2003; Millard *et al*. 2008). However, the response of root and microbial respiration to heavy precipitation in permafrost region is not clear.

In the permafrost region, heavy precipitation would affect not only the CO_2 flux from the soil but also the exchange of GHGs CH_4 and N_2O. Generally, natural oxic soil absorbs CH_4 (Potter *et al.* 1996). Striegl *et al.* (1992) reported that a precipitation on dry soil increased CH_4 consumption by the soil. Liu *et al.* (2008) reported that CH_4 fluxes showed little difference between the irrigated and non-irrigated soils in an Inner Mongolian steppe soil. van Huissteden *et al.* (2008) reported that CH_4 consumption in a forest near Yakutsk remained stable even when the water table fluctuated from 9 to 27 cm. This indicates that methanotrophs occur in the uppermost soil and fluctuation in soil moisture do not affect on CH_4 consumption in the forest of this region.

Very few studies have reported the effect of precipitation on N_2O emission from boreal forests. Rodionow *et al.* (2006) reported that emission of N_2O is negligible from natural Siberian soils. Forest soil near Yakutsk emit or absorb little N_2O (Morishita *et al.*

2007; Takakai *et al.* 2008). Du *et al.* (2006) reported that N_2O emission was stimulated by precipitation events in natural grassland in Inner Mongolia.

The purpose of this study was to evaluate the effect of heavy precipitation on GHG fluxes from soil in Taiga forest near Yakutsk by conducting an irrigation experiment. In this study, we measured GHG production rates both in the O-layer and the mineral soil, microbial respiration, and root respiration separately to evaluate the effect of precipitation on global warming potential of the soil in this ecosystem in detail.

MATERIALS AND METHODS

Site description

This study was conducted during July 2004 in a 180-year-old larch forest on sandy loam soil underlain by permafrost (Typic Haploturbels, Soil Survey Staff 2010) in Spasskaya-Pad experimental forest (62˚15' N, 129˚37' E) of the Institute for Biological Problems of Cryolithozone, near Yakutsk, Russia. The site is located on a gently sloped (1 to 2^{o} decline toward north) terrace around 200 m in elevation situated on the left bank of the Lena River. The mean annual temperature is -10.0 ºC and the mean annual precipitation is around 237 mm (Japan Meteorological Agency 2004). The amount of precipitation in 2004 preceding the experiment was lower than the mean precipitation for 30 years (Fig. 1). This indicates that the forest floor was relatively dry during the experiment. The forest is mainly occupied by larch trees (*Larix cajanderi*). The forest floor is covered by shrubby vegetation including *Vaccinium vitis-idaea* and *Arctous erythrocarpa* and by a thick 10 cm organic layer (O-layer).

The precipitation amount during the period from June 17th to July 26th 2003 was recorded by a rain gauge (Young Inc., USA) at the top of a 32 m-high scaffolding tower built by Ohta *et al.* (2001).

Layout of experimental plots

An irrigated plot and a non-irrigated plot of the same size (14 x 14 m^2) were established. The non-irrigated plot was established in the area more than 50 m apart from the irrigated plot not to be affected by irrigation (Fig. 2). Four sub-plots of size 0.16 m^2 were set up in the spring of 2003 in each irrigated and non-irrigated plot. Around each sub-plot, the outside edges of 0.16 m^2 were trenched. The trenches were made approximately 30 cm deep into the soil, which is enough to prevent invasion of roots of Siberian larch because we estimated from soil profile examination that about 97% of fine roots (< 2 mm in diameter) was distributed within the -10 to 26 cm depth of the soil (Table 1: Ono 2003). The trenches were lined with plastic sheets before backfilling to prevent root growth. Aboveground parts of all vegetation were removed from the trenched plots.

Irrigation was carried out between 17:00 and 21:00 from 17th to 22nd July 2004. Irrigation was accomplished by using a rubber hose from approximately 1.5 m height. The irrigation of 20 mm per day was conducted every day and a total of 120 mm of irrigation was applied. The amount of irrigation was approximately equal to the average amount of natural precipitation including heavy precipitation events during the summer season (June to September). The Lena River water was used for the irrigation. The temperature of the water irrigated was about 15 ºC.

Field measurements

CO_2 fluxes from the surface of the O-layer (R_s) were measured using a closed chamber method (Kusa *et al.* 2008, Morishita *et al.* 2005, 2006, 2007, Takakai *et al.* 2008) from

1st to 23rd July 2004. In order to measure R_s including root and microbial respiration, four stainless steel cylinders, approximately 20 cm in diameter and 25 cm height, were installed at a 4 cm depth into the soil both in the irrigated and non-irrigated plots at least 24 h before the measurement. Aboveground parts of all plants inside the cylinders were removed carefully to exclude plant respiration. Before starting the measurements, an air sample inside the cylinder was transferred into Tedlar® bags as a 0-min sample, and an acrylic lid with silicone gasket and an inflatable plastic bag to adjust air pressure inside the chamber was put on the cylinder immediately. Six minutes later, a 500 ml air sample inside the chambers was taken out. Each chamber remained open for more than 10 min after completion of the CO_2 flux measurement to allow a complete exchange of air inside the chamber. Gas samples were then taken for measuring CH_4 and N_2O fluxes on the surface of the O-layer. At 0, 30, and 60 min after the top of the chamber was again closed with a lid, a 20 ml gas sample inside the chamber was taken into a 10 ml vacuum vial sealed with a butyl rubber stopper (SVF-10, Nichiden-Rika, Kobe, Japan).

One stainless steel cylinder was installed in the middle of each trenched plot in both the irrigated and non-irrigated plots in four replicates to measure the rate of microbial respiration in the whole soil (R_{mw}). The measurements were performed on the same day of gas sampling. The procedure for measuring R_{mw} was same as the CO_2 measurement.

Stainless steel pipes of 9 mm in diameter were installed at depths of 10, 20, 30, and 50 cm (four pipes at each depth) out of the trenched plot in both the irrigated and non-irrigated plots in the spring of 2003 to collect air samples in the soil. The pipes were sealed by three-way cocks to allow gas concentration in the pipes to equilibrate with the soil air. From each of the pipes installed at each depth and each treatment, air samples (50 ml) were taken into a Tedlar^R bag during the chamber measurements. All samples that were taken from the same depth and treatment were mixed into a Tedlar^R bag. Air samples of 50 ml from each of the Tedlar^R bags were diluted with CO_2-free air for CO_2 analysis, and 20 ml were transferred to 10 ml glass bottles for CH_4 and N_2O analysis.

These measurements were conducted between 10:00 and 18:00 to avoid diurnal effects on fluxes. We did not carry out measurements within 12 h from irrigation in order to avoid effects of the physical movement of water in the soil.

During the chamber measurements, air and soil temperature, and soil moisture around each chamber were recorded manually. Air temperature around each chamber was measured with digital thermometers to calculate GHG fluxes. Two replications of soil temperature measurement at the depth of 10 cm near each chamber, which is the boundary between the O-layer and the mineral soil, was also conducted with digital thermometers. Two replications of soil moisture measurement as volumetric water content at the 0-10 cm depth of soil (O-layer) on each chamber base was conducted with a calibrated TDR sensor (time domain reflectometer; TRIME-como, Tohoku Electronic Industrial Co. Ltd., Sendai, Japan).

Soil temperature and moisture were recorded automatically in about 5 m away from each chamber in both the irrigated and non-irrigated plots (Lopez *et al*. 2007). Soil temperature was measured using the calibrated thermistors at depths of 10, 20, 30, 40, and 60 cm (T_{10}, T_{20}, T_{30}, T_{40}, and T_{60}, respectively; 104ET, Ishizuka Denshi, Tokyo, Japan). Because of some sensor troubles with a thermistor at the depth of 20 cm, we excluded the T_{20} data from the analysis. The thermistors were calibrated using an ice-water bath with a precision of 0.02°C at 0°C; the overall probe accuracy for the temperature range of -20 to 30 °C was calculated to be better than ±0.09 °C. T_{10} was recalibrated using soil temperature measured manually around chambers. Soil moisture was measured using an FDR (Frequency Domain Reflectometry) method at depths of 0-10, 10-20, 20-30, 30-40, and 50-60 cm (W_{10}, W_{20}, W_{30}, W_{40}, and W_{60}, respectively; EnviroSMART, Sentek Pty Ltd., Australia, respectively). The FDR sensors were calibrated separately for 0-10 cm and below 10 cm depths (mineral soil layer). For this purpose, we collected 11 *in situ* soil samples of each soil depth with various moisture conditions, and determined the volumetric water content gravimetrically to construct a calibration curve. W_{10} was recalibrated using soil moisture measured manually around the chambers. Soil temperature was recorded every 30 seconds and stored every 1 h on average while soil moisture was recorded every 1 h. The soil temperature and moisture recorded at the time of gas sampling were used for statistical analyses.

Physical and chemical conditions of soil and water samples

In order to analyze the physical properties, three soil cores of size 100 cm^3 were sampled from each layer divided in 2003. With these undisturbed cores, we measured the volume of the air-filled pore space (AFPS) using a three phase meter (Model DIK-1110, Daiki Rika Kogyo Do. Ltd.). The gas tortuosity factor (D/D_0) of undisturbed soil cores were measured and calculated by using the method developed by Osozawa and Kubota (1987) under steady-state conditions using O_2 as the diffusing gas. The cores were oven-dried (105 ºC) for 48 h to obtain bulk density and water-filled pore space (WFPS). The porosity was calculated as the sum of WFPS and AFPS. Length of fine roots (< 2 mm in diameter) in each layer was calculated using a theoretical equation after Ono (2003) as follows:

$$R = \frac{2n}{S}$$

where R is the length of fine roots in a unit volume of each layer (cm cm^{-3}; Table 1); n is the number of the cut ends of fine roots appearing on each layer in the soil profile; S is the area of each layer in the soil profile (cm^{-2}).

The fresh soil samples were sieved (2 mm) and were used for the chemical analysis. The concentrations of NO_3^--N in a 1:20 for the O-layer and a 1:10 for the mineral soil: deionized water mixture was measured using ion chromatography (TOA DIC Analyzer ICA-2000, TOA DKK, Tokyo, Japan). The concentrations of NH_4^+-N in a 1:20 for the O-layer and a 1:10 for the mineral soil: 1 mol L^{-1} KCl solution mixtures were measured using colorimetry (the indophenol-blue method) with a UV-VIS spectrophotometer (UV mini 1240, Shimadzu, Kyoto, Japan).

The irrigated water was sampled directly from the rubber hose which was used to apply irrigation water. Rain water was sampled using eight rain gutters (0.12 m^2 each) put around the irrigated and non-irrigated plots.

Concentrations of NH_4^+-N and NO_3^--N in irrigation as well as rain water were also measured. Contents of NH_4^+-N and NO_3^--N in soil were calculated multiplying the bulk density and NH_4^+-N or NO_3^--N concentration of each layer of the soil. Contents of NH_4^+-N and NO_3^--N in irrigation and rain water were calculated multiplying the amount of irrigation or rain water and NH_4^+-N or NO_3^--N concentrations of the water.

Analysis of CO_2, CH_4, and N_2O concentrations

The CO_2 concentration was determined with a portable infrared CO_2 gas analyzer (ZFP9GC11; Fuji Electric systems Co. Ltd., Tokyo, Japan). CH_4 and N_2O concentrations were analyzed using gas chromatography equipped with a flame ionization detector and an electron capture detector, respectively (GC-8A and GC-14B, Shimadzu, Kyoto, Japan).

Estimation of soil-gas diffusivity and calculation of flux, respiration, and production rates of greenhouse gases

Greenhouse gas fluxes, measured by a closed chamber method, were calculated as follows:

$$F_c = \rho \times \frac{V}{A} \times \frac{dc}{dt} \times \frac{273}{273 + T}$$

where F_c is the flux of GHGs obtained from the closed chamber method (μg C or N m^{-2} h^{-1}); ρ is the gas density of GHGs (CO_2-C, CH_4-C: 0.536 × 10^3 g m^{-3}, N_2O-N: 1.25 × 10^3 g m^{-3}); V/A is the height of the chamber (m); dc/dt is the ratio of change in the gas concentration (c) inside the chamber per unit time (t) during the sampling period (m^3 m^{-3} h^{-1}); and T is the air temperature (ºC).

We estimated the flux of each GHG from the mineral soil to the O-layer using a soil gradient method (Kusa *et al.* 2008). The soil-gas diffusivities were estimated using the soil AFPS (Fig. 3). Estimated diffusivities were corrected for temperature effects using $D_T/D_{25} = [(273+T) / 298]^{1.75}$ (Reid *et al*. 1977). Greenhouse gas flux from the mineral soil to the O-layer was determined from Fick's law as:

$$F_d = - D \frac{dc}{dz}$$

where F_d is the flux obtained from Fick's law (μg C or N cm^{-2} s^{-1}), D is the soil gas coefficient (cm^2 s^{-1}) at the surface of the mineral soil calculated using the gas tortuosity factor (D/D_0) and the molecular diffusivity of each GHG in air (D_{0CO2} = 0.138, D_{0CH4} =

0.191, D_{0N2O} = 0.143), dc/dz is the ratio of change in the gas concentration (c) along the soil depth (z) (μg C or N cm^{-3} cm^{-1}). We made quadratic functions of depth (10, 20, 30, and 50 cm) to each GHG concentration to calculate dc/dz at the 10-cm depth, the boundary between the O-layer and the mineral soil, as the slope of the tangent to the quadratic functions at the 10-cm depth (Takle *et al.* 2004). We did not use the data of GHG concentration at the 0-cm depth, ambient air, to make the quadratic functions because there is always some variation in the gas concentrations due to the turbulent mixing of ambient air and to some extent the topmost O-layer (Pihlatie *et al.* 2007).

The root respiration rate (R_r) of each measurement was calculated as the difference between CO_2 flux from the surface of the O-layer in the root-intact (R_s) and trenched plots (the microbial respiration rate in the whole soil (R_{mw})) of each measurement. One negative value of R_r was eliminated. We regarded the estimated GHG fluxes from the mineral soil into the O-layer as GHG production rates in the mineral soil assuming no movement of GHGs in the permafrost. The GHG production rates in the O-layer were calculated as the difference between the GHG fluxes from the surface of the O-layer and the production rates of GHG in the mineral soil to avoid problems caused by the turbulent mixing of ambient air and the unevenly distributed O-layer constituents (Davidson & Trumbore 1995; Pihlatie *et al.* 2007; Schwendenmann & Veldkamp 2006).

For CO_2, we regarded the CO_2 production rates in the mineral soil as the microbial respiration rates in the mineral soil (R_{mm}) assuming almost all R_r was occurring in the O-layer because most part of fine roots were distributed in the O-layer (Table 1). The microbial respiration rate in the O-layer (R_{mo}) was calculated as the difference between the R_{mw} and R_{mm}.

The following equations were applied to the measured temperature and CO_2 flux or production rate data (F_{CO2}) to calculate the normalized CO_2 flux or the production rate ($F_{CO2,\,b}$) corresponding to the base temperature (T_b, 5 °C in the present study):

$$F_{CO2} = a \times \exp(b \times T)$$

$$F_{CO2,\,b} = F_{CO2} \times \exp\left[b \times \left(T_b - T\right)\right]$$

where a and b are fitted constants and T is soil temperature at the 10-cm depth (Takakai *et al.* 2008).

Negative fluxes and production rates of CH_4 and N_2O represent the downward movement or net consumption of the gases.

To evaluate the relative significance of CO_2, CH_4, and N_2O, their global warming potentials (GWP; mg CO_2-eq m^{-2} h^{-1}) expressed in CO_2-equivalent values were calculated by multiplying the CO_2, CH_4, and N_2O fluxes by 44/12, 16/12*25, and 44/28*298, respectively (100-year time horizon; IPCC 2007).

Statistical analyses

Two-way analysis of variance (ANOVA) or paired t-test was performed to compare average GHG fluxes, productions, soil temperature, or soil moisture obtained from the irrigated and non-irrigated plots on each before and during the irrigation period.

Linear or non-linear regression analyses were performed to examine the relationship between the measured GHG flux and production, soil temperature, and moisture. Spearman's correlation analyses were performed to examine the relationship between W_{20} and other variables because of the non-normal distribution of W_{20}.

A multiple regression analysis was carried out to evaluate the contributions of R_r, R_{mo}, R_{mm}, CH_4 production in the O-layer and the mineral soil, and N_2O production in the O-layer and the mineral soil to GWP.

Significance for all statistical analyses was accepted at P = 0.05. All statistical analyses were performed with the statistical package R version 2.9.1 (R Development Core Team 2009).

RESULTS

Physical and chemical properties of soil

The soil physical and chemical properties are shown in Table 1. The dry bulk density in the O-layer was 0.41 and that in the mineral soil ranged from 1.1 to 1.9 Mg m^{-3}, and increased with an increase in depth. The porosity in the mineral soil ranged from 0.34 to 0.55 m^3 m^{-3} and D/D_0 in the mineral soil before the irrigation experiment ranged from 0.01 to 0.11 m^2 s^{-1}, and both decreased with an increase in depth. NO_3^--N and NH_4^+-N concentrations in each layer ranged from 0.02 to 0.23 mg kg $soil^{-1}$ and 0.00 to 0.02 g kg $soil^{-1}$, respectively and both were highest in the O-layer whereas there was no trend in the mineral soil. NH_4^+-N contents in the O-layer and the mineral soil (1-62 cm) were 816 and 9160 mg m^{-2}, respectively and NO_3^--N contents were 9 and 82 mg m^{-2}, respectively. The estimated length of fine roots in each layer ranged from 0 to 80 m L^{-1} and 86% of the fine roots were distributed in the O-layer.

Precipitation, soil temperature, and soil moisture

A total of 11.4 mm of precipitation occurred during 30 days before the irrigation period. The amount of precipitation from 17th June to 27th July was 19.8 mm.

Soil temperature at depths of 10, 30, 40, and 60 cm (T_{10}, T_{30}, T_{40}, and T_{60}, respectively) during flux measurements ranged from -0.5 to 7.6 ºC in the irrigated plot and from -0.0 to 6.9 ºC in the non-irrigated plot (Fig. 4A, B). Before the irrigation period, the average soil temperature at each depth in the irrigated plot was significantly lower than that in the non-irrigated plot (Table 2; $P < 0.01$). During the irrigation period, the average T_{10} in the irrigated plot was significantly higher than that in the non-irrigated plot ($P < 0.01$), the average T_{60} in the irrigated plot was significantly lower than that in the non-irrigated plot ($P < 0.001$), and the average T_{30} and T_{40} were not different between the irrigated and non-irrigated plots.

Soil moisture in the O-layer (W_{10}) during the flux measurements ranged from 0.11 to 0.14 m^3 m^{-3} in the irrigated plot and from 0.10 to 0.13 m^3 m^{-3} in the non-irrigated plot (Fig. 4C, D). Soil moisture at depths of 10-20, 20-30, 30-40, and 50-60 cm (W_{20}, W_{30}, W_{40}, and W_{60}, respectively) ranged from 0.13 to 0.31 m^3 m^{-3} in the irrigated plot and from 0.10 to 0.16 m^3 m^{-3} in the non-irrigated plot. The soil moisture increased with an increase in depth in both plots. Although average soil moisture at each depth in the irrigated plot was significantly higher than that in the non-irrigated plot both before and during the irrigation period (Table 2; $P < 0.01$), soil moisture in the irrigated plot tended to increase with an increase in irrigation (Fig. 4D). W_{20} in the irrigated plot was significantly higher during the irrigation period than before the irrigation period and W_{20} in the non-irrigated plot was significantly lower during the irrigation period than before the irrigation period (both at $P < 0.001$).

Nitrogen supply by irrigation and precipitation

The NH_4^+-N and NO_3^--N concentrations in irrigation water were 0.09 and 0.10 mg L^{-1} and that in rain water were 0.14 and 0.005, respectively. The NH_4^+-N and NO_3^--N supply to the soil by irrigation were 11 and 12 mg m^{-2} and that by rain water were 2.8 and 0.1, respectively. A total of 13.8 mg m^{-2} of NH_4^+-N and 12.1 of NO_3^--N were added to the soil during the measurement period.

Greenhouse gas flux from the surface of the O-layer

The CO_2 flux from the surface of the O-layer in the root-intact plot (R_s) ranged from 59 to 200 mg C m^{-2} h^{-1} in the irrigated plot and from 70 to 142 in the non-irrigated plot, and both fluctuated with the variation in soil temperature (Fig. 4A, B, 5A). Before the irrigation period, average R_s (mean ± standard deviation [SD]) in the irrigated plot (106±32 mg C m^{-2} h^{-1}; Table 2) was not different from that in the non-irrigated plot (116±21). During the irrigation period, average R_s in the irrigated plot (171±20) was significantly higher than that in the non-irrigated plot (109±11; P < 0.001). The CO_2 flux from the surface of the O-layer in the trenched plot (microbial respiration rate in whole soil; R_{mw}) ranged from 50 to 132 mg C m^{-2} h^{-1} in the irrigated plot and from 54 to 109 in the non-irrigated plot, and those accounted for 42 – 108% (mean ± SD; 67±12%) of R_s (Fig. 5B). This percentage was high in the beginning of the measurement period and decreased with time. Before the irrigation period, average R_{mw} (mean ± SD) in the irrigated plot (67±15 mg C m^{-2} h^{-1}; Table 2) was significantly lower than that in the non-irrigated plot (80±15; P < 0.05). During the irrigation period, average R_{mw} in the irrigated plot (122±10) was significantly higher than that in the non-irrigated plot (63±6; P < 0.001).

The ranges of the root respiration rate (R_r), calculated from the difference between R_s and R_{mw}, were 26 – 90 and 12 – 53 mg C m^{-2} h^{-1} in the irrigated and non-irrigated plots, respectively and those accounted for 17 – 58% (mean ± SD; 35±9%) of R_s (Fig. 5C). This percentage was low in the beginning of the measurement period and increased with an increase in soil temperature in the non-irrigated plot whereas irrigation depressed the rate in the irrigated plot. The average R_r in the irrigated plot was not different from that in the non-irrigated plot before and during the irrigation period (Table 2).

The CH_4 flux from the surface of the O-layer ranged from -15 to -0 μg C m^{-2} h^{-1} in the irrigated plot and from -22 to -1 in the non-irrigated plot (Fig. 6A). Before the irrigation period, the average CH_4 flux (mean ± SD) in the irrigated plot (-8.3±3.4 μg C m^{-2} h^{-1}; Table 2) was not different from that in the non-irrigated plot (-8.3±3.5). During the irrigation period, the CH_4 flux in the irrigated plot (-5.4±4.1) was significantly higher than that in the non-irrigated plot (-14.0±6.5; $P < 0.001$).

The N_2O flux from the surface of the O-layer ranged from -0.9 to 3.9 μg N m^{-2} h^{-1} in the irrigated plot and from -1.7 to 3.8 in the non-irrigated plot (Fig. 6B). Before the irrigation period, the average N_2O flux (mean ± SD) in the irrigated plot (0.13±0.63 μg N m^{-2} h^{-1}; Table 2) was not different from that in the non-irrigated plot (1.21±1.56 μg N m^{-2} h^{-1}). During the irrigation period, the N_2O flux in the irrigated plot (1.58±1.64 μg N m^{-2} h^{-1}) was significantly higher than that in the non-irrigated plot (0.21±1.12 μg N m^{-2}

h^{-1}; $P < 0.05$).

Greenhouse gas concentration in the soil

The ranges of CO_2 concentration of soil air at the depth of 10, 20, 30, and 50 cm were 720 – 4740 ppmv in the irrigated plot and 900 – 3600 ppmv in the non-irrigated plot (Fig. 7A, B). The CO_2 concentrations increased with an increase in depth in both plots.

The ranges of CH_4 concentration of soil air at the depth of 10, 20, 30, and 50 cm were 0.30 – 2.07 ppmv in the irrigated plot and 0.34 – 2.16 ppmv in the non-irrigated plot (Fig. 7C, D). The CH_4 concentration decreased with an increase in depth in both plots.

The ranges of N_2O concentration of soil air at the depth of 10, 20, 30, and 50 cm were 0.30 – 0.33 ppmv in the irrigated plot and 0.29 – 0.33 ppmv in the non-irrigated plot (Fig. 7E, F). The N_2O concentration was independent from the depth of soil in both plots.

Greenhouse gas production rate

The ranges of the microbial respiration rate in the O-layer (R_{mo}) were 29 – 105 and 40 – 80 mg C m^{-2} h^{-1} in the irrigated and non-irrigated plots, respectively and those accounted for 26 – 62% (mean ± SD; 50±9%) of R_s (Fig. 8A). This percentage was high in the beginning of the measurement period and decreased with an increase in soil temperature in the non-irrigated plot whereas irrigation enhanced the rate in the irrigated plot. Before the irrigation period, average R_{mo} (mean ± SD) in the irrigated plot (44±16 mg C m^{-2} h^{-1}; Table 2) was significantly lower than that in the non-irrigated plot (64±13; P < 0.001). During the irrigation period, average R_{mo} in the irrigated plot (97±8 mg C m^{-2} h^{-1}) was significantly higher than that in the non-irrigated plot (54±5; P < 0.001). The microbial respiration rate in the mineral soil (R_{mm}) ranged from 18 to 29 mg C m^{-2} h^{-1} in the irrigated plot and from 5 to 22 mg C m^{-2} h^{-1} in the non-irrigated plot, and those accounted for 5 – 49% (mean ± SD; 16±9%) of R_s (Fig. 8A). This percentage was high in the beginning of the measurement period and decreased with time. The average R_{mm} before and during the irrigation period (mean ± SD) in the irrigated plot were 24±4 and 25±2 mg C m^{-2} h^{-1} and both were significantly higher than that in the non-irrigated plot (17±3 and 9±3 mg C m^{-2} h^{-1}, respectively; P < 0.01; Table 2).

CH_4 production rate in the O-layer ranged from -4 to 11 µg C m^{-2} h^{-1} in the irrigated plot and -13 to 12 in the non-irrigated plot (Fig. 8B). Before the irrigation period, average CH_4 production rate in the O-layer (mean ± SD) in the irrigated plot (3.6±4.3 μg C m^{-2} h^{-1}; Table 2) was not different from that in the non-irrigated plot (3.8±5.4). During the irrigation period, the CH_4 production rate in the irrigated plot (6.1±4.0) was significantly higher than that in the non-irrigated plot (-5.7±6.3; $P < 0.05$). The CH_4 production rate in the mineral soil ranged from -17 to -8 μg C m^{-2} h^{-1} in the irrigated plot and -17 to -5 in the non-irrigated plot (Fig. 8B). Average CH_4 production rate in the mineral soil in the irrigated plot was not different from that in the non-irrigated plot before and during the irrigation period (Table 2).

N_2O production rate in the O-layer ranged from -1.0 to 3.8 μg N m^{-2} h^{-1} in the irrigated plot and -1.7 to 3.6 μg N m^{-2} h^{-1} in the non-irrigated plot. The N_2O production rate in the mineral soil ranged from -0.2 to 0.6 μg N m^{-2} h^{-1} in the irrigated plot and -0.6 to 0.5 in the non-irrigated plot (Fig. 8C). Average N_2O production rates in both the O-layer and the mineral soil in the irrigated plot were not different from that in the non-irrigated plot before and during the irrigation period (Table 2).

Global warming potentials

Before the irrigation period, global warming potential (GWP) of the soil (mean ± SD) in the irrigated plot (390±117 mg CO_2-eq m^{-2} h^{-1}) was not different from that in the non-irrigated plot (425±78). During the irrigation period, the GWP in the irrigated plot (628±75) was significantly higher than that in the non-irrigated plot (398±39; $P < 0.001$; Table 3). CO_2 production accounted for more than 99% of the GWP in both the irrigated and non-irrigated plots both before and during the irrigation period. The GWP increment due to irrigation was mainly caused by an increase in microbial respirations. R_{mo} had the greatest contribution on GWP in both the irrigated and non-irrigated plots both before and during the irrigation period. The GWP by only CH_4 and N_2O production during the irrigation period in the non-irrigated plot was negative (-0.20 mg CO_2-eq m^{-2} h^{-1}) because CH_4 consumption by the soil offset the GWP by N_2O production. However, the GWP in the irrigated plot was positive (0.56 mg CO_2-eq m^{-2} h^{-1}) mainly due to an increase in GWP by N_2O production which could not be offset by CH_4 consumption.

Controlling factors for GHG fluxes

Non-linear regressions revealed a significant positive correlation between T_{10} and R_s, R_r, R_{mw}, and R_{mo} (r = 0.87, 0.53, 0.68, and 0.72, respectively, $P < 0.01$; Fig. 9A, D, G, J). No significant correlation between T_{10} and R_{mm} was also obtained (r = 0.11; Fig. 12A). The normalized R_{mw} and R_{mm} were significantly and positively correlated with W_{10} and W_{20}, respectively, whereas normalized R_r was significantly and negatively correlated with W_{10} (r = 0.64, 0.76, and -0.38, respectively, $P \leq 0.05$; Fig. 9F, I, 12C). The normalized R_{mo} had a weak positive correlation with W_{10} (r = 0.36, $P = 0.07$; Fig. 9L). Both the CH_4 flux from the surface of the O-layer and the CH_4 production rate in the O-layer had significant positive correlations with W_{10} (r = 0.60 and 0.62, respectively, $P < 0.001$; Fig. 10B, D). The CH_4 production rate in the mineral soil was not correlated with either T_{10} or W_{20} (Fig. 12D, E). Each N_2O flux or N_2O production rate did not significantly correlate with either soil temperature or moisture (Fig. 11, 12F, G). The N_2O flux from the surface of the O-layer had a significant positive correlation with R_{mw} (r = 0.45, $P < 0.05$; Fig. 13).

We carried out multiple regression analyses to evaluate the contributions of R_r, R_{mo}, R_{mm}, CH_4 production in the O-layer and the mineral soil, and N_2O production in the O-layer and the mineral soil to GWP (Table 4). The results showed that R_{mo} had the largest effect on the GWP followed by R_r and R_{mm}. This indicates that microbial activity would play an important role in controlling GWP of the soil in this region. CH_4 and N_2O production rates had a little effect on the GWP.

DISCUSSION

Effects of irrigation on soil temperature and moisture

Both soil temperature at a 10-cm depth (temperature of boundary between the O-layer and the mineral soil; T_{10}) and soil moisture in the O-layer (W_{10}) increased by irrigation (Fig. 4B, D). The increase in T_{10} would be due to a higher temperature of irrigation water (approximately 15 ºC) than T_{10} in the irrigated plot before the irrigation period (4.5 ºC in average). The temperature of raindrops should be in the balance between latent heat by evaporation of raindrops and sensible heat from the atmosphere to raindrops (Ogura 1999). Anderson *et al.* (1998) verified that measured raindrop temperature and wet-bulb temperature were almost equal. Mean temperature of raindrop in July in Yakutsk is calculated at 14 ºC from mean air temperature (18.7 ºC) and mean relative humidity (60%) in July in Yakutsk (Japan Meteorological Agency 2004). These indicate that an increase in soil temperature due to heavy precipitation would occur in this region. Permafrost creates a strong heat sink in the summer that keeps soil temperature low (Eugster *et al.* 2000) and therefore soil temperature would increase greatly due to heavy precipitation events in this region. The reason why the precipitation during the experiment period had not affected the soil temperature (Fig. 4) could be the very low amount of precipitation in one event (2.2 mm in maximum).

Effects of irrigation on CO_2 flux and CO_2 production rate

The increase in R_{mo} due to irrigation was affected by the soil temperature in our study (Fig. 9J), which is consistent with a previous study (e.g. Boone *et al*. 1998). On the other hand, the normalized R_{mo} had only a weak positive effect on the soil moisture (Fig. 9L). These results indicate that the increase in R_{mo} was mainly caused by the increase in soil temperature due to irrigation. Generally, microbial respiration rate increases immediately after irrigation in dry condition whereas the microbial respiration rate did not vary or decrease due to irrigation in wet enough condition (Howard & Howard 1993). The weak relationship between the soil moisture and normalized R_{mo} indicated that the O-layer in this site was in relatively dry condition but not in severely dry condition. Waldrop & and Zak (2006) mentioned that there was a trend that the soil amended with NO_3^--N (7 mg kg soil^{-1}) could enhance soil C decomposition rate within 1.5 times. Comparing the supply of NH_4^+-N and NO_3^--N to the soil by irrigation (11 and 12 mg N m^{-2}, respectively) with NH_4^+-N and NO_3^--N contents in the O-layer (826 and 9 mg N m^{-2}, respectively), NH_4^+-N supply could be negligible whereas NO_3^--N supply was equivalent to 1.3 times the NO_3^--N content in the O-layer. However, an increase in NO_3^--N concentrations in the O-layer due to irrigation could not exceed 0.3 mg kg $soil^{-1}$ (Table 1). Therefore it appeared that the NO_3^--N amendment of soil by the irrigation water hardly affected the R_{mo}.

There was no significant correlation between the soil temperature and R_{mm} (Fig. 12A). On the other hand, both R_{mm} and normalized R_{mm} were significantly and positively affected by the soil moisture (Fig. 12B, C). W_{20} in the irrigated plot was significantly higher during the irrigation period than before the irrigation period, and W_{20} in the non-irrigated plot was significantly lower during the irrigation period than before the irrigation period (both at $P < 0.001$). This indicates that the change in W_{20} could be the reason of lower R_{mm} during the irrigation period in the non-irrigated plot compared to that in the irrigated plot, even if there were no differences between R_{mm} in the non-irrigated and irrigated plots before the irrigation period. NH_4^+-N and NO_3^--N content in the mineral soil (9160 and 82 mg N m^{-2}, respectively) were much higher than those in the O-layer (826 and 9 mg N m^{-2}, respectively), so that the effect of inflow of nitrogen from the O-layer into mineral soil due to the irrigation to R_{mm} was negligible.

As a result, the positive correlation between soil temperature and R_{mw} (Fig. 9D) was derived from the positive correlation between soil temperature and R_{mo}. On the other hand, the positive correlation between soil moisture and normalized R_{mw} (Fig. 9F) was derived mainly from the positive correlation between soil moisture and R_{mm}. These indicated that future increase in heavy precipitation events in summer resulting in increase in soil temperature and moisture could accelerate the decomposition of soil C in the O-layer as well as in the mineral soil.

Irrigation did not increase the root respiration rate (R_r) in our study whereas a negative correlation between normalized R_r and soil moisture and a positive correlation between R_r and soil temperature were observed (Fig. 5C, 9G, I). A very few studies reported the effect of irrigation or precipitation accompanied by an increase in soil moisture on R_r. R_r was depressed by surplus water due to reduced diffusion of oxygen in soil (Bouma & Bryla 2000). A positive relationship between soil temperature and R_r is reported in many studies (Atkin *et al.* 2000; Pregitzer *et al.* 2000). The increase in percentage of R_r to R_s with soil temperature in the non-irrigated plot in our study strongly supported a positive correlation between soil temperature and R_r. These results indicate that a negative effect of the increase in soil moisture due to irrigation on R_r offset the positive effect of the increase in soil temperature on R_r in this ecosystem. It is suggested that the soil in active layer investigated was too wet not to increase R_r

accompanied by an increase in soil temperature due to a shortage of oxygen during the irrigation period.

The R_s in this study was positively correlated with soil temperature which increased with an increase in irrigation (Fig. 9A). A positive relationship between soil temperature and R_s is reported in many studies (Boone *et al.* 1998; Davidson *et al.* 1998; Xu & Qi 2001). On the other hand, the normalized R_s was not affected by an increase in soil moisture due to irrigation (Fig. 9C). We concluded that an increase in soil moisture due to irrigation in this study accelerated R_{mw} whereas depressed R_r. Consequently, the soil moisture appeared to have no influence on R_s. This indicates that the permafrost in this region would have a potential to supply an adequate amount of water to plants (Sugimoto *et al.* 2002) whereas would not have a potential to keep high soil moisture that depress decomposition of the soil organic matter.

Effects of irrigation on CH_4 flux and CH_4 production rate

The CH_4 flux from the surface of the O-layer in this study (from -22 to -0 μg C m^{-2} h^{-1}) ranged in a higher rate than the reported values in forests in northern Europe (from -143 to -1 μg C m^{-2} h^{-1}; Smith *et al*. 2000). Outside the permafrost region in Russia, Nakano *et al.* (2004) reported the CH_4 flux ranging from -210 to -69 μg C m^{-2} h^{-1} in western Siberia and Morishita *et al.* (2005) reported the CH_4 flux of -63 μg C m^{-2} h^{-1} near Khabarovsk. Those fluxes are much lower than the fluxes we obtained. On the other hand, in a permafrost region of Russia, Morishita *et al.* (2006) reported the CH_4 flux ranging from -3.4 to -1.6 μg C m^{-2} h^{-1} in central Siberia and Takakai *et al.* (2008) reported the range from -10 to 3.4 μg C m^{-2} h^{-1} near Yakutsk, which are similar to our results. Flessa *et al.* (2008) mentioned that the lower CH_4 consumption in soils with continuous permafrost can be explained by factors that hamper diffusion of atmospheric CH_4 into the soil. However, van Huissteden *et al.* (2008) observed the CH_4 flux ranging from -301 to -278 μg C m^{-2} h^{-1} in a forest only 1 km off our study site. The reason for this variation is unknown.

The CH_4 production rate in the mineral soil was lower than that in the O-layer in this study. This result is similar to that of the previous studies (Dong *et al*. 1998; Saari *et al*. 1998).

The CH_4 production rate in the mineral soil was not different between the irrigated and non-irrigated plots despite the difference in soil moisture in these plots (Fig. 8B, 12E). CH_4 production rate in the soil is the net result of simultaneously occurring production and consumption of CH_4 within the soil (Butterbach-Bahl & Papen 2002;

Yavitt *et al*. 1995). This indicates that the potential for both gross CH_4 production and consumption rates in the mineral soil did not change along with the increase in soil moisture due to the irrigation.

On the other hand, the increase in CH_4 production rate in the O-layer due to irrigation was affected by the soil moisture in our study (Fig. 10D). In the irrigated plot, the CH_4 production rates in the O-layer were positive during the irrigation period. This would indicate that the increase in CH_4 production in the O-layer due to irrigation in our study would be caused by a change in balance between gross CH_4 production consumption rates in the O-layer due to an increase in soil moisture. The CH_4 production rates in the O-layer were estimated from the two kinds of fluxes measured with different methods, so that these rates include much assumption. However, there is a possibility that a significantly higher CH_4 flux from the surface of the O-layer in the irrigated plot compared to that in the non-irrigated plot during the irrigation period (Fig. 6A) was resulted by the change in the CH_4 production rate in the O-layer, because the CH_4 production rate in the mineral soil was not affected by the irrigation. The effect of the addition of NH_4^+ by irrigation water should not be significant because NH_4^+ content in the O-layer was much higher than that added by the irrigation (826 and 11 mg N m^{-2}, respectively). Generally, a negative correlation between soil moisture and CH_4 flux is observed in a dry condition and a positive correlation between them is observed in a wet condition (Curry 2007; Striegl *et al.* 1992). In our study, soil dryness was not a limiting factor for CH_4 consumption.

Effects of irrigation on N_2O flux and N_2O production rate

The N_2O flux from the surface of the O-layer (from -1.7 to 3.9 μg N m^{-2} h^{-1}) ranged in a lower rate of reported values in boreal forests (from -4.9 to 22.3; Dalal & Allen 2008). Previous studies conducted near Yakutsk also reported very low values (from -2.1 to 4.6; Morishita *et al.* 2007, Takakai *et al.* 2008). These low values show characteristics of an N limited region (Hatano *et al.* 2001; Schulze *et al.* 1995). The result of much larger N_2O production in the O-layer than that in the mineral soil observed in this study was consistent with that of the previous studies (Saari *et al.* 1997).

Some studies reported a positive correlation between soil moisture and temperature and N_2O flux from the surface of the O-layer in natural forests (e.g. Dong *et al.* 1998; Fest *et al.* 2009). Although the N_2O flux during the irrigation period in our study was higher in the irrigated plot than that in the non-irrigated plot, the N_2O fluxes did not correlate with either soil moisture or temperature (Fig. 11, 12E, F). Only a weak positive correlation between the N_2O flux from the surface of the O-layer and soil temperature was found (P = 0.08). Both the N_2O production rates in the O-layer and the mineral soil were not different between the irrigated and non-irrigated plots both before and during the irrigation period and did not correlate significantly with either soil moisture or soil temperature. On the other hand, the N_2O flux from the surface of the O-layer was positively correlated with both R_{mw} (P < 0.05; Fig. 13). This indicates that the main cause of an increase in N_2O flux from the surface of the O-layer due to irrigation was not a direct effect of both soil temperature and moisture but an indirect effect of microbial activities. Comparing NH_4^+-N and NO_3^--N supply to the soil by irrigation (11 and 12 mg N m^{-2}, respectively) with NH_4^+-N and NO_3^--N contents in the O-layer which produced most of N_2O on the whole soil (826 and 9 mg N m^{-2}, respectively), NH_4^+-N supply could be negligible whereas NO_3^--N supply was comparable with NO_3^--N content in the O-layer. This indicates that NO_3^--N supply by irrigation might stimulate N_2O emission *via* increase in denitrification in the irrigated plot. Liu *et al.* (2008) could not detect a variation in N_2O flux from the surface of the O-layer after irrigation due to the lack of substrate for denitrification process on grassland in Inner Mongolia. The weak relationship between N_2O flux from the surface of the O-layer and both soil temperature and moisture in this study might be caused by deficiency of nitrogen. Du *et al.* (2006) also observed no significant linear relationship between both soil temperature and moisture and diurnal N_2O flux from the surface of the O-layer in grassland in Inner Mongolia. However, they mentioned that it was the distribution of effective precipitation, rather than precipitation intensity, which influenced seasonal and inter-annual variations in N_2O flux. Even in the ecosystem investigated in this study, it is necessary to observe for a long period to examine the effects of precipitation on N_2O flux from the surface of the O-layer.

Conclusions

In the investigated Taiga forest near Yakutsk, which is characterized by low soil temperature and dry weather, heavy precipitation events would increase both soil temperature and moisture. The increased soil temperature and moisture would accelerate microbial activities, which play an important role in controlling the GWP in the soil resulting in decomposition of soil organic matter in both the O-layer and the mineral soil. As a result, release of inorganic nitrogen into the soil together with an increase in N_2O emission, which has a huge impact on the GWP of the soil, would be expected. Continuous study on the effect of change in precipitation pattern on decomposition of soil organic matter accompanied by N mineralization is very crucial in predicting future GWP of the soil in this region. In addition, an increase in gross CH_4 production rate might decrease a potential for CH_4 sink of the soil. Further study is required to investigate the change in CH_4 production in the O-layer caused by heavy rain events.

ACKNOWLEDGMENTS

We are deeply thankful to the staff members of the Institute for Biological Problems of Cryolithozone, Siberian Branch, Russian Academy of Science for their support during the field research. This study was funded by the RR2002 Program of the Japanese Ministry of Education, Culture, Sports, Science and Technology.

REFERENCES

Anderson SP, Hinton A, Weller RA 1998: Moored observations of precipitation temperature. *Journal of Atmospheric and Oceanic Technology* **15,** 979-986.

Atkin OK, Edwards EJ, Loveys BR 2000: Response of root respiration to changes in temperature and its relevance to global warming. *New Phytol.*, **147**, 141-154.

Bond-Lamberty B, Wang CK, Gower ST 2004: A global relationship between the heterotrophic and autotrophic components of soil respiration? *Global Change Biol.*, **10**, 1756-1766.

Boone RD, Nadelhoffer KJ, Canary JD, Kaye JP 1998: Roots exert a strong influence on the temperature sensitivity of soil respiration. *Nature*, **396**, 570-572.

Borken W, Davidson EA, Savage K, Gaudinski J, Trumbore SE 2003: Drying and wetting effects on carbon dioxide release from organic horizons. *Soil Sci. Soc. Am. J.*, **67**, 1888-1896.

Bouma TJ, Bryla DR 2000: On the assessment of root and soil respiration for soils of different textures: interactions with soil moisture contents and soil CO_2 concentrations. *Plant Soil*, **227**, 215-221.

Butterbach-Bahl K, Papen H 2002: Four years continuous record of CH_4-exchange between the atmosphere and untreated and limed soil of a N-saturated spruce and beech forest ecosystem in Germany. *Plant Soil*, **240**, 77-90.

Curry CL 2007: Modeling the soil consumption of atmospheric methane at the global scale. *Global Biogeochem. Cycles*, **21**, -.

Dalal RC, Allen DE 2008: Greenhouse gas fluxes from natural ecosystems. *Aust. J. Bot.*,

56, 369-407.

Davidson EA, Belk E, Boone RD 1998: Soil water content and temperature as independent or confounded factors controlling soil respiration in a temperate mixed hardwood forest. *Global Change Biol.*, **4**, 217-227.

Davidson EA, Trumbore SE 1995: Gas Diffusivity and Production of CO_2 in Deep Soils of the Eastern Amazon. *Tellus Series B-Chemical and Physical Meteorology* **47**, 550-565.

Dong Y, Scharffe D, Lobert JM, Crutzen PJ, Sanhueza E 1998: Fluxes of CO_2, CH_4 and N_2O from a temperate forest soil: the effects of leaves and humus layers. *Tellus Series B-Chemical and Physical Meteorology*, **50**, 243-252.

Du R, Lu DR, Wang GC 2006: Diurnal, seasonal, and inter-annual variations of N_2O fluxes from native semi-arid grassland soils of inner Mongolia. *Soil Biology & Biochemistry*, **38**, 3474-3482.

Easterling DR, Evans JL, Groisman PY *et al*. 2000: Observed variability and trends in extreme climate events: A brief review. *Bulletin of the American Meteorological Society* **81**, 417-425.

Eugster W, Rouse WR, Pielke RA *et al.* 2000: Land-atmosphere energy exchange in Arctic tundra and boreal forest: available data and feedbacks to climate. *Global*

Change Biol., **6**, 84-115.

Fest BJ, Livesley SJ, Drosler M, van Gorsel E, Arndt SK 2009: Soil-atmosphere greenhouse gas exchange in a cool, temperate Eucalyptus delegatensis forest in south-eastern Australia. *Agricultural and Forest Meteorology*, **149**, 393-406.

Flessa H, Rodionov A, Guggenberger G *et al.* 2008: Landscape controls of CH_4 fluxes in a catchment of the forest tundra ecotone in northern Siberia. *Global Change Biol.*, **14**, 2040-2056.

Goodale CL, Apps MJ, Birdsey RA *et al.* 2002: Forest carbon sinks in the Northern Hemisphere. *Ecol. Appl.*, **12**, 891-899.

Hatano R, Sawamoto T, Shibuya M *et al.* 2001: Characteristics of Nitrogen Cycling in Permafrost Regional Ecosystems in Yakutsk, Russia. In: Fukuda M & Kobayashi Y (eds) *Ninth Symposium on the Joint Siberian Permafrost Studies between Japan and Russia in 2000*, pp 99-103. Sapporo, Japan.

Howard DM, Howard PJA 1993: Relationships between CO_2 Evolution, Moisture-Content and Temperature for a Range of Soil Types. *Soil Biology & Biochemistry*, **25**, 1537-1546.

IPCC 2007: *Climate change 2007: The Physical Science Basis. Contribution of Working Group I to the Fourth Assessment Report of the Intergovernmental Panel on*

Climate Change, Cambridge University Press, Cambridge, United Kingdom and New York, NY, USA.

Japan Meteorological Agency 2004: *Monthly report of the Japan Meteorological Agency*, Japan Meteorological Agency, Tokyo.

Kusa K, Sawamoto T, Hu R, Hatano R 2008: Comparison between closed-chamber and gas concentration gradient methods for measurement of CO_2 and N_2O fluxes in two upland field soils. *Soil Sci. Plant Nutr.*, **54**, 777-785.

Liu CY, Holst J, Bruggemann N *et al.* 2008: Effects of Irrigation on Nitrous Oxide, Methane and Carbon Dioxide Fluxes in an Inner Mongolian Steppe. *Advances in Atmospheric Sciences*, **25**, 748-756.

Lopez MLC, Saito H, Kobayashi Y *et al.* 2007: Interannual environmental-soil thawing rate variation and its control on transpiration from *Larix cajanderi*, Central Yakutia, Eastern Siberia. *Journal of Hydrology*, **338**, 251-260.

Millard P, Midwood AJ, Hunt JE, Whitehead D, Boutton TW 2008: Partitioning soil surface CO_2 efflux into autotrophic and heterotrophic components, using natural gradients in soil delta C-13 in an undisturbed savannah soil. *Soil Biology & Biochemistry*, **40**, 1575-1582.

Morishita T, Hatano R, Desyatkin RV 2007: N2O Flux in Alas Ecosystems Formed by

Forest Disturbance Near Yakutsk, Eastern Siberia, Russia. *Eurasian Journal of Forest Research*, **10**, 79-84.

Morishita T, Hatano R, Takahashi K, Kondrashov LG 2005: Effect of Deforestation on CH_4 Uptake in Khabarovsk, Far East, Russia. *Phyton*, **45**, 267-274.

Morishita T, Matsuura Y, Zyryanova OA, Abaimov AP 2006: CO_2, CH_4, and N_2O fluxes from a larch forest soil in Central Siberia. In: Hatano R & Guggenberger G (eds) *Symptom of Environmental Change in Siberian Permafrost Region*, pp 1-9. Hokkaido University Press, Sapporo, Japan.

Nakano T, Inoue G, Fukuda M 2004: Methane consumption and soil respiration by a birch forest soil in West Siberia. *Tellus Series B-Chemical and Physical Meteorology*, **56**, 223-229.

Oberbauer SF, Gillespie CT, Cheng W, *et al*. 1992: Environmental-Effects on CO_2 Efflux from Riparian Tundra in the Northern Foothills of the Brooks Range, Alaska, USA. *Oecologia* **92**, 568-577.

Ogura Y 1999: *General Meteorology* (in Japanese), University of Tokyo Press, Tokyo.

Ohta T, Hiyama T, Tanaka H *et al.* 2001: Seasonal variation in the energy and water exchanges above and below a larch forest in eastern Siberia. *Hydrological Processes*, **15**, 1459-1476.

Ono R 2003: Examination of presuming method of the length of the line contained in a space, and the application in investigation of tea plant rootlet (in Japanese with English summary). *Root Research*, **12**, 119-123.

Osozawa S, Kubota T 1987: Method or measuring soil gas diffusion coefficient (in Japanese). *Japanese Journal of Soil Science and Plant Nutrition*, **58**, 528-535.

Pihlatie M, Pumpanen J, Rinne J et al. 2007: Gas concentration driven fluxes of nitrous oxide and carbon dioxide in boreal forest soil. *Tellus Series B-Chemical and Physical Meteorology* **59**, 458-469.

Potter CS, Davidson EA, Verchot LV 1996: Estimation of global biogeochemical controls and seasonality in soil methane consumption. *Chemosphere,* **32**, 2219-2246.

Pregitzer KS, King JA, Burton AJ, Brown SE 2000: Responses of tree fine roots to temperature. *New Phytol.*, **147**, 105-115.

R Development Core Team 2009: *R: A language and environment for statistical computing*, R Foundation for Statistical Computing, Vienna, Austria, URL: http://www.R-project.org.

Reid RC, Prausnitz JM, Sherwood TK 1977: *The properties of gases and liquids,* McGraw-Hill, New York.

Rodionow A, Flessa H, Kazansky O, Guggenberger G 2006: Organic matter composition and potential trace gas production of permafrost soils in the forest tundra in northern Siberia. *Geoderma*, **135**, 49-62.

Saari A, Heiskanen J, Martikainen PJ 1998: Effect of the organic horizon on methane oxidation and uptake in soil of a boreal Scots pine forest. *FEMS Microbiol. Ecol.*, **26**, 245-255.

Saari A, Martikainen PJ, Ferm A *et al.* 1997: Methane oxidation in soil profiles of Dutch and Finnish coniferous forests with different soil texture and atmospheric nitrogen deposition. *Soil Biology & Biochemistry*, **29**, 1625-1632.

Schwendenmann L, Veldkamp E 2006: Long-term CO_2 production from deeply weathered soils of a tropical rain forest: evidence for a potential positive feedback to climate warming. *Global Change Biol.* **12,** 1878-1893.

Schulze ED, Schulze W, Kelliher FM *et al.* 1995: Aboveground Biomass and Nitrogen Nutrition in a Chronosequence of Pristine Dahurian Larix Stands in Eastern Siberia. *Canadian Journal of Forest Research-Revue Canadienne De Recherche Forestiere*, **25**, 943-960.

Sirotenko OD, Abashina EV 2008: Modern Climate Changes of Biosphere Productivity in Russia and Adjacent Countries. *Russian Meteorology and Hydrology*, **33**, 267-271.

Smith KA, Dobbie KE, Ball BC *et al.* 2000: Oxidation of atmospheric methane in Northern European soils, comparison with other ecosystems, and uncertainties in the global terrestrial sink. *Global Change Biol.*, **6**, 791-803.

Soil Survey Staff 2010: Soil taxonomy. A basic system of soil classification for making and interpreting soil surveys 11th ed., US Gov. Printing Office, Washington, DC.

Striegl RG, Mcconnaughey TA, Thorstenson DC, Weeks EP, Woodward JC 1992: Consumption of Atmospheric Methane by Desert Soils. *Nature*, **357**, 145-147.

Sugimoto A, Yanagisawa N, Naito D, Fujita N, Maximov TC 2002: Importance of permafrost as a source of water for plants in east Siberian taiga. *Ecol. Res.* **17,** 493-503.

Takakai F, Desyatkin AR, Lopez CML, Fedorov AN, Desyatkin RV, Hatano R 2008: Influence of forest disturbance on CO_2, CH_4 and N_2O fluxes from larch forest soil in the permafrost taiga region of eastern Siberia. *Soil Sci. Plant Nutr.*, **54**, 938-949.

Takle ES, Massman WJ, Brandle JR *et al.* 2004: Influence of high-frequency ambient pressure pumping on carbon dioxide efflux from soil. *Agricultural and Forest Meteorology*, **124**, 193-206.

van Huissteden J, Maximov TC, Kononov AV, Dolman AJ 2008: Summer soil CH_4

emission and uptake in taiga forest near Yakutsk, Eastern Siberia. *Agricultural and Forest Meteorology*, **148**, 2006-2012.

Waldrop MP, Zak DR 2006: Response of oxidative enzyme activities to nitrogen deposition affects soil concentrations of dissolved organic carbon. *Ecosystems* **9**, 921-933.

Xu M, Qi Y 2001: Soil-surface CO_2 efflux and its spatial and temporal variations in a young ponderosa pine plantation in northern California. *Global Change Biol.*, **7**, 667-677.

Yavitt JB, Fahey TJ, Simmons JA 1995: Methane and Carbon-Dioxide Dynamics in a Northern Hardwood Ecosystem. *Soil Sci. Soc. Am. J.* **59**, 796-804.

Figure captions

Figure 1 Seasonal variation in air temperature and precipitation in Yakutsk. Open and closed circles indicate average air temperature for each month in 30 years and in 2004, respectively. Open and closed bars indicate average precipitation for each month in 30 years and the amount of precipitation for each month in 2004, respectively.

Figure 2 Location map of the study site and layout of the measurement plots. Microbial respiration in the whole soil was measured in the trenched plots. Fluxes and concentrations of GHGs in soil air were measured nearby the trenched plots.

Figure 3 Effect of soil air-filled pore space on the measured gas tortuosity factor (diffusivity relative to that for still air). Symbols distinguish measurements on soil cores from different layers.

Figure 4 Temporal variation in soil temperature at 10, 30, 40, and 60 cm depths (T_{10}, T_{30}, T_{40}, and T_{60}, respectively; A, B) and soil moisture at 0-10, 10-20, 20-30, 30-40, and 50-60 cm depths (W_{10}, W_{20}, W_{30}, W_{40}, and W_{60}, respectively; C, D) of the non-irrigated (A, C) and irrigated plots (B, D). Arrows indicate the irrigation events for the irrigated plot. Open bars represent the precipitation amount.

Figure 5 Temporal variation in CO_2 fluxes from the surface of the O-layer (R_s; A), microbial respiration from the surface of the O-layer (R_{wm}; B), and root respiration (R_r; C). Open symbols indicate the data from the non-irrigated plot and closed symbols indicate the data from the irrigated plot. Vertical bars denote the standard error of each parameter. Arrows indicate the irrigation events for the irrigated plot.

Figure 6 Temporal variation in CH_4 fluxes from the surface of the O-layer (A) and N_2O fluxes from the surface of the O-layer (B) of the non-irrigated (open symbols) and irrigated plots (closed symbols). Positive values indicate net emission and negative values indicate net consumption. Vertical bars denote the standard error of each parameter. Arrows indicate the irrigation events for the irrigated plot.

Figure 7 Temporal variation in CO_2 (A, B), CH_4 (C, D), and N_2O (E, F) concentrations in soil air at 10, 20, 30, and 50 cm depths of the non-irrigated (A, C, E) and irrigated plots (B, D, F). Data from 10, 20, 30, and 50 cm depths are indicated by open circles, closed circles, open triangles, and closed triangles, respectively. Arrows indicate the irrigation events for the irrigated plot. Open bars represent the precipitation amount.

Figure 8 Temporal variation in microbial respiration rate in the O-layer and the mineral soil (R_{mo} are indicated by circles and R_{mm} are indicated by triangles; A), CH_4 production rates in the O-layer and the mineral soil (circles and triangles, respectively; B), and N_2O production rates in the O-layer and the mineral soil (circles and triangles, respectively; C) of the non-irrigated (open symbols) and irrigated plots (closed symbols). Positive values indicate net emission and negative values indicate net consumption. Arrows indicate the irrigation events for the irrigated plot.

Figure 9 CO_2 fluxes from the surface of the O-layer (R_s; A, B), microbial respiration from the surface of the O-layer (R_{wm}; D, E), root respiration (R_r; G, H), microbial respiration rate in the O-layer (R_{mo}; J, K), and normalized R_s, R_{wm}, R_r, and R_{mo} (C, F, I, L) plotted against soil temperature at the 10 cm depth (A, D, G, J) and moisture at the

0-10 cm depth (B, C, E, F, H, I, K, L). Open and closed circles indicate the data of non-irrigated and irrigated plots before irrigation and open and closed triangles indicate the data of non-irrigated and irrigated plots during irrigation. $^{\dagger}P < 0.1$; $*P \leq 0.05$; $**P < 0.01$; $***P < 0.001$. Vertical bars denote the standard error of each parameter.

Figure 10 CH_4 fluxes from the surface of the O-layer (A, B) and CH_4 production rate in the O-layer (C, D) plotted against soil temperature at the 10 cm depth (A, C) and moisture at the 0-10 cm depths (B, D). Open and closed circles indicate the data of non-irrigated and irrigated plots before irrigation and open and closed triangles indicate the data of non-irrigated and irrigated plots during irrigation. $***P < 0.001$. Vertical bars denote the standard error of each parameter.

Figure 11 N_2O fluxes from the surface of the O-layer (A, B) and N_2O production rate in the O-layer (C,D) plotted against soil temperature at the 10 cm depth (A, C) and moisture at the 0-10 cm depth (B, D). Open and closed circles indicate the data of non-irrigated and irrigated plots before irrigation and open and closed triangles indicate the data of non-irrigated and irrigated plots during irrigation. $^{\dagger}P < 0.1$. Vertical bars denote the standard error of each parameter.

Figure 12 Microbial respiration rate in mineral soil (A, B), CH_4 (C, D), and N_2O production rates in mineral soil (E, F) plotted against soil temperature at the 10 cm depth (A, C, E) and moisture at the 0-10 cm depth (B, D, F). Open and closed circles indicate the data of non-irrigated and irrigated plots before irrigation and open and closed triangles indicate the data of non-irrigated and irrigated plots during irrigation. *$P < 0.05$; ***$P < 0.001$. The coefficient values written in italics are calculated by Spearman's correlation analysis. Vertical bars denote the standard error of each parameter.

Figure 13 CO_2 fluxes from the surface of the O-layer (R_s) plotted against N_2O fluxes from the surface of the O-layer. Open and closed circles indicate the data of non-irrigated and irrigated plots before irrigation and open and closed triangles indicate the data of non-irrigated and irrigated plots during irrigation. $^*P < 0.05$. Vertical and horizontal bars denote the standard error of the R_s and N_2O fluxes, respectively.

Table captions

Table 1 Soil physical and chemical properties at the study site

[†]O: O-layer (thickness of O-layer was 10 cm); A and B: Mineral soil layers (with organic matter and illuviation, respectively); Ca: Accumulation of carbonate.

[‡]D/D_0: Gas tortuosity factor.

[§]Length of fine roots (< 2 mm in diameter) was calculated after Ono (2003).

¶SiL: Silty loam; L: Loam; SL: Sandy loam.

Table 2 Average greenhouse gas fluxes, production, global warming potentials and soil temperature and moisture during each period of the measurement†

Within the group of GHG fluxes, productions, and soil temperature and moisture, values with different letters are significantly different at the 0.05 level.

†R_s: soil respiration rate, R_r: root respiration rate, R_{mw}, R_{mo}, R_{mm}: microbial respiration rate from whole soil, O-layer, and mineral soil, respectively, CH_4(w), CH_4(o), CH_4(m): CH_4 production rate in whole soil, O-layer, and mineral soil, respectively, N_2O(w), N_2O(o), N_2O(m): N_2O production rate in whole soil, O-layer, and mineral soil, respectively, T_i: soil temperature at i cm depth, W_i: soil moisture at i cm depth.

Table 3 Average global warming potentials of root respiration (R_r), microbial respiration in the O-layer (R_{mo}), microbial respiration in the mineral soil (R_{mm}), and CH_4 and N_2O production of each part of the soil in each period (expressed in CO_2-equivqlent; mg CO_2-eq m^{-2} h^{-1}) from the study site. Positive values indicate net production and negative values indicate net consumption by the soil.

Within the group of GHG fluxes, productions, and soil temperature and moisture, values with different letters are significantly different at the 0.05 level.

Table 4 Standardized partial regression coefficients obtained from a multiple regression analysis to evaluate the contributions of R_r, R_{mo}, R_{mm}, CH_4 production in the O-layer and the mineral soil, and N_2O production in the O-layer and the mineral soil to GWP†

†R_r: root respiration rate, R_{mo}, R_{mm}: microbial respiration rate from the O-layer and mineral soil, respectively, CH_4(o), CH_4(m): CH_4 production rate in the O-layer and mineral soil, respectively, N_2O(o), N_2O(m): N_2O production rate in the O-layer and mineral soil, respectively, GWP: global warming potential.

Layer[†]	Depth cm	Bulk density $Mg\ m^{-3}$	Porosity $m^3\ m^{-3}$	D/D_0[‡]	NO_3-N conc. mgN kg $soil^{-1}$	NH_4-N conc. gN kg $soil^{-1}$	Length of fine roots[§] $cm\ cm^{-3}$	Soil texture[¶]
O	0 ~ 10	0.41	-	-	0.228	0.020	8.0	-
A	~ 25	1.10	0.55	0.11	0.023	0.005	0.6	SCL
B_1	~ 36	1.55	0.41	0.03	0.140	0.006	0.4	SL
B_{21}	~ 50	1.63	0.40	0.07	0.094	0.005	0.1	LS
B_{22Ca}	~ 72	1.52	0.37	0.06	0.101	0.018	0.2	SL
B_{23}	~ 78	1.65	0.39	0.11	-	-	0.0	LS
B_{3Ca}	~ 91	1.86	0.34	0.01	-	-	0.0	SL

		Before irrigation period		During irrigation period	
		Non-irrigated plot	Irrigated plot	Non-irrigated plot	Irrigated plot
R_s	mg C m^{-2} h^{-1}	116 ± 21^a	106 ± 32^a	109 ± 11^a	171 ± 20^b
R_r	mg C m^{-2} h^{-1}	36 ± 11^a	45 ± 23^a	45 ± 8^a	49 ± 14^a
R_{mw}	mg C m^{-2} h^{-1}	80 ± 15^b	67 ± 15^a	63 ± 6^a	122 ± 10^b
R_{mo}	mg C m^{-2} h^{-1}	64 ± 13^b	44 ± 16^a	54 ± 5^a	97 ± 8^b
R_{mm}	mg C m^{-2} h^{-1}	17 ± 3^a	24 ± 4^b	9 ± 3^a	25 ± 2^b
CH_4(w)	μg C m^{-2} h^{-1}	-8.3 ± 3.4^a	-8.3 ± 3.5^a	-14.0 ± 6.5^a	-5.4 ± 4.1^b
CH_4(o)	μg C m^{-2} h^{-1}	3.8 ± 5.4^a	3.6 ± 4.3^a	-5.67 ± 6.3^a	6.1 ± 4.0^b
CH_4(m)	μg C m^{-2} h^{-1}	-12.0 ± 3.3^a	-11.9 ± 2.4^a	-8.4 ± 1.9^a	-11.5 ± 2.4^a
N_2O(w)	μg N m^{-2} h^{-1}	1.21 ± 1.56^a	0.13 ± 0.63^a	0.21 ± 1.12^a	1.58 ± 1.64^b
N_2O(o)	μg N m^{-2} h^{-1}	1.06 ± 1.52^a	0.06 ± 0.63^a	0.32 ± 1.11^a	1.44 ± 1.71^a
N_2O(m)	μg N m^{-2} h^{-1}	0.15 ± 0.22^a	0.07 ± 0.19^a	-0.11 ± 0.26^a	0.14 ± 0.26^a
T_{10}	^{0}C	5.53 ± 1.04^b	5.06 ± 1.43^a	6.92 ± 0.60^a	7.63 ± 0.28^b
T_{20}	^{0}C	7.62 ± 1.68^b	4.92 ± 1.18^a	7.76 ± 0.46^b	6.77 ± 0.46^a
T_{30}	^{0}C	4.61 ± 1.09^b	2.97 ± 0.89^a	4.84 ± 0.21^a	5.09 ± 0.52^a
T_{40}	^{0}C	3.12 ± 0.90^b	1.60 ± 0.76^a	3.54 ± 0.19^a	3.69 ± 0.52^a
T_{60}	^{0}C	1.22 ± 0.79^b	-0.08 ± 0.30^a	1.93 ± 0.07^b	1.18 ± 0.49^a
W_{10}	m^3 m^{-3}	0.12 ± 0.01^a	0.13 ± 0.01^b	0.10 ± 0.00^a	0.12 ± 0.00^b
W_{20}	m^3 m^{-3}	0.12 ± 0.00^a	0.24 ± 0.01^b	0.11 ± 0.00^a	0.26 ± 0.00^b
W_{30}	m^3 m^{-3}	0.15 ± 0.00^a	0.24 ± 0.00^b	0.14 ± 0.00^a	0.26 ± 0.01^b
W_{40}	m^3 m^{-3}	0.15 ± 0.00^a	0.21 ± 0.01^b	0.15 ± 0.00^a	0.24 ± 0.01^b
W_{60}	m^3 m^{-3}	0.13 ± 0.02^a	0.22 ± 0.03^b	0.16 ± 0.02^a	0.28 ± 0.02^b

	Before irrigation period		During irrigation period	
	Non-irrigated plot	Irrigated plot	Non-irrigated plot	Irrigated plot
R_r	131[a] (31%)	166[a] (43%)	167[a] (42%)	180[a] (29%)
R_{mo}	233[b] (55%)	163[a] (42%)	198[a] (50%)	355[b] (56%)
R_{mm}	61[a] (14%)	86[b] (22%)	34[a] (8%)	93[b] (15%)
CH_4 production in O-layer	0.125[a] (0.03%)	0.122[a] (0.03%)	-0.188[a] (-0.05%)	0.202[b] (0.03%)
CH_4 production in mineral soil	-0.401[a] (-0.09%)	-0.397[a] (-0.10%)	-0.280[a] (-0.07%)	-0.383[a] (-0.06%)
N_2O production in O-layer	0.496[a] (0.12%)	0.029[a] (0.01%)	0.150[a] (0.04%)	0.674[a] (0.11%)
N_2O production in mineral soil	0.069[a] (0.02%)	0.031[a] (0.01%)	-0.051[a] (-0.01%)	0.064[a] (0.01%)
Net GWP	425[a] (100%)	390[a] (100%)	398[a] (100%)	628[b] (100%)

	Standardized partial regression coefficient
R_r	0.474
R_{mo}	0.695
R_{mm}	0.212
CH_4(o)	0.002
CH_4(m)	0.001
N_2O(o)	0.005
N_2O(m)	0.001

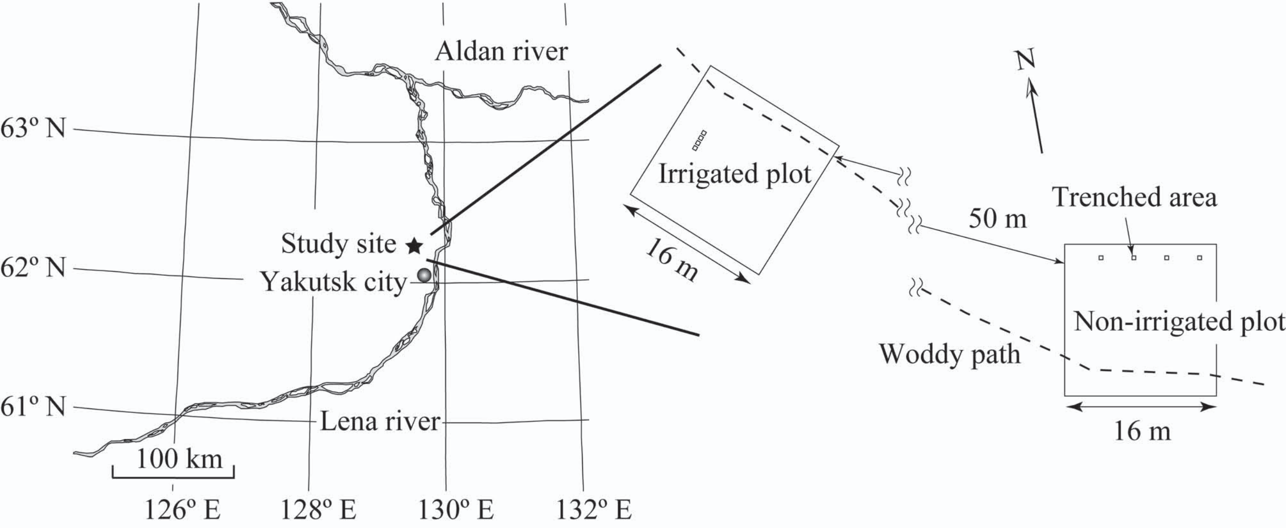
Aldan river
63º N
62º N
61º N
Study site
Yakutsk city
Lena river
100 km
126º E
128º E
130º E
132º E
N
Irrigated plot
16 m
50 m
Trenched area
Non-irrigated plot
Woddy path
16 m

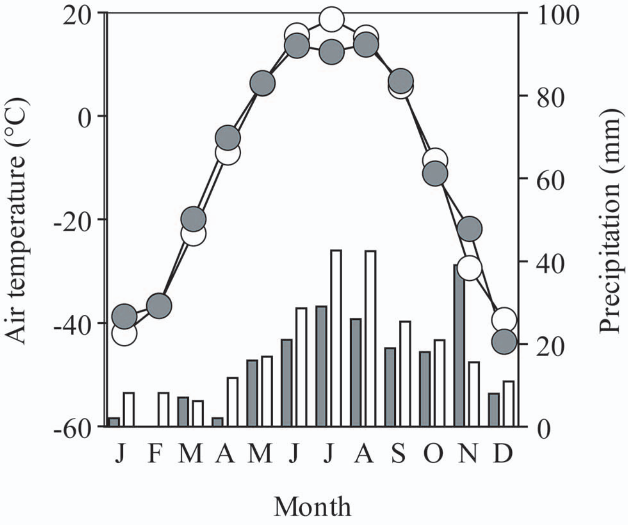

20
0
-20
-40
-60
Air temperature (°C)
100
80
60
40
20
0
Precipitation (mm)
J
F
M
A
M
J
J
A
S
O
N
D
Month

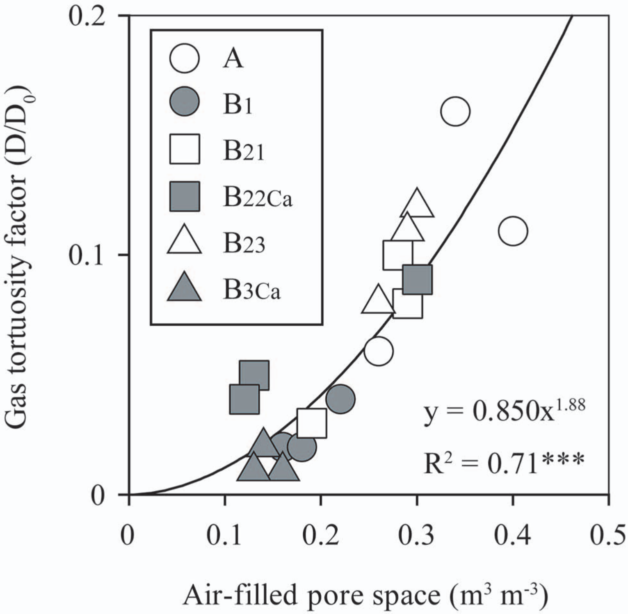

Gas tortuosity factor (D/D0)
Air-filled pore space (m3 m-3)
A
B1
B21
B22Ca
B23
B3Ca
y = 0.850x1.88
R2 = 0.71***
0
0.1
0.2
0.3
0.4
0.5

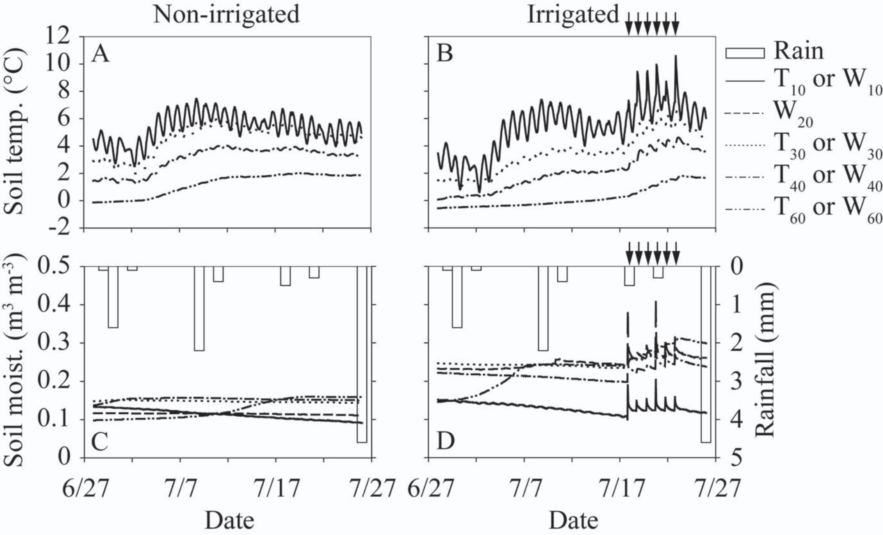

Non-irrigated
Irrigated
A
B
C
D
Soil temp. (°C)
Soil moist. (m3 m-3)
Rainfall (mm)
Rain
T10 or W10
W20
T30 or W30
T40 or W40
T60 or W60
Date
Date
6/27
7/7
7/17
7/27

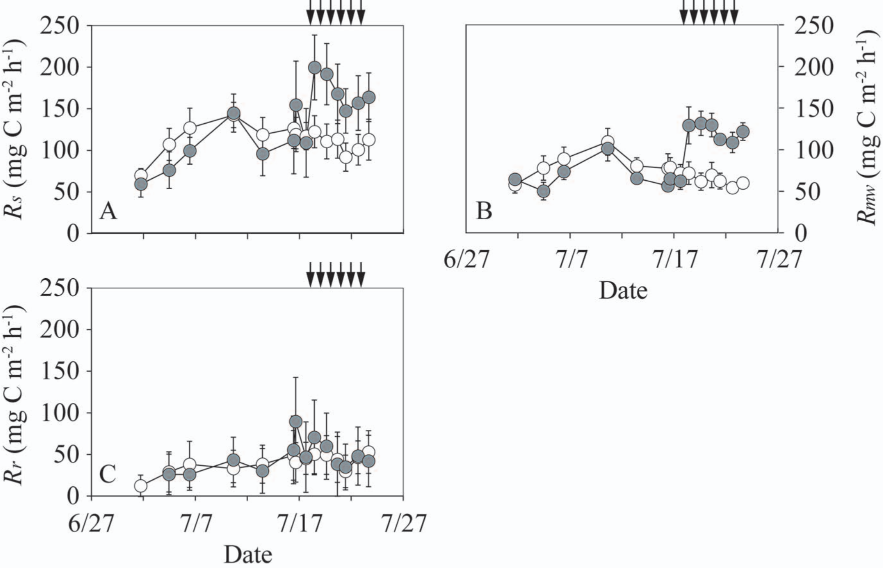

250
200
150
100
50
0
Rs (mg C m-2 h-1)
A
B
Rmw (mg C m-2 h-1)
C
Rr (mg C m-2 h-1)
6/27
7/7
7/17
7/27
Date

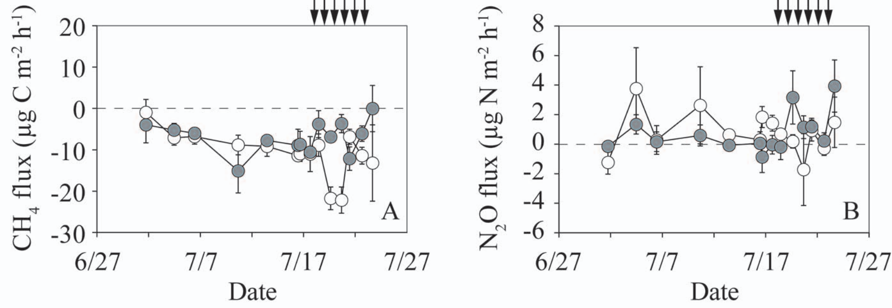

CH4 flux (µg C m-2 h-1)
20
10
0
-10
-20
-30
A
6/27
7/7
7/17
7/27
Date
N2O flux (µg N m-2 h-1)
8
6
4
2
0
-2
-4
-6
B
6/27
7/7
7/17
7/27
Date

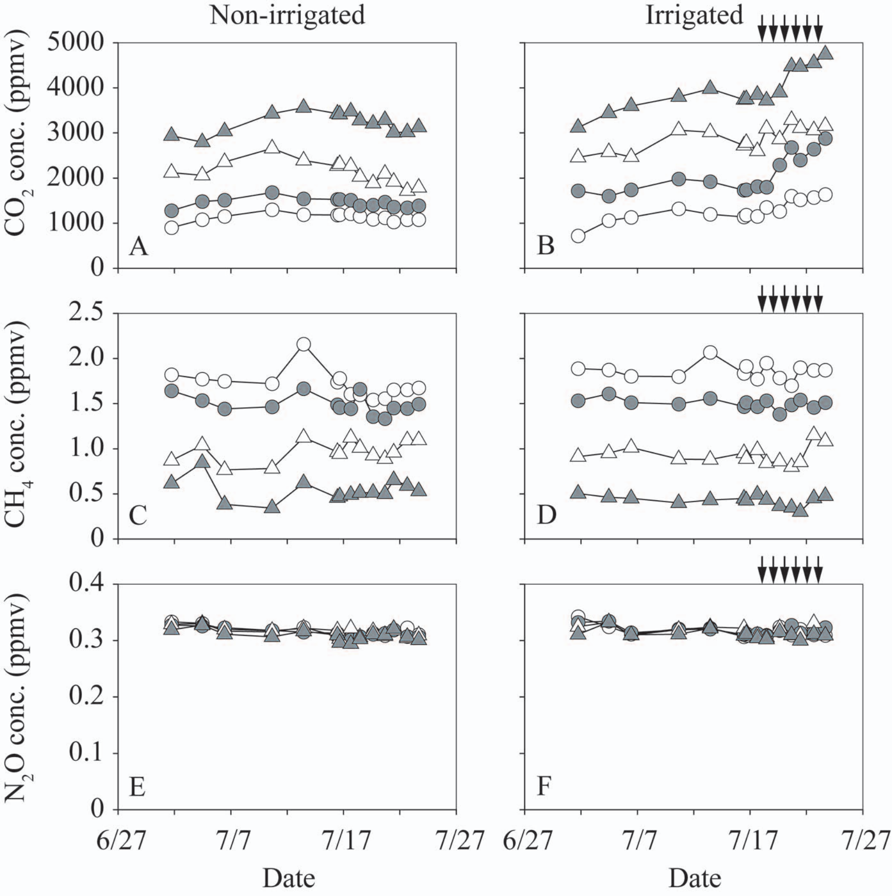

Non-irrigated
Irrigated
CO_2 conc. (ppmv)
5000
4000
3000
2000
1000
0
A
B
CH_4 conc. (ppmv)
2.5
2.0
1.5
1.0
0.5
0
C
D
N_2O conc. (ppmv)
0.4
0.3
0.2
0.1
0
E
F
6/27
7/7
7/17
7/27
Date

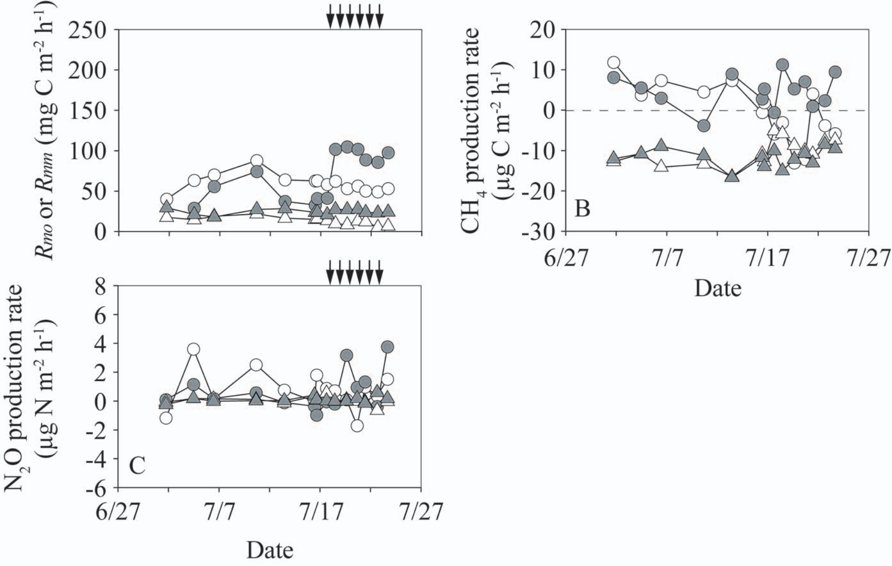

Rmo or Rmm (mg C m-2 h-1)
250
200
150
100
50
0
CH4 production rate (μg C m-2 h-1)
20
10
0
-10
-20
-30
B
6/27
7/7
7/17
7/27
Date
N2O production rate (μg N m-2 h-1)
8
6
4
2
0
-2
-4
-6
C
6/27
7/7
7/17
7/27
Date

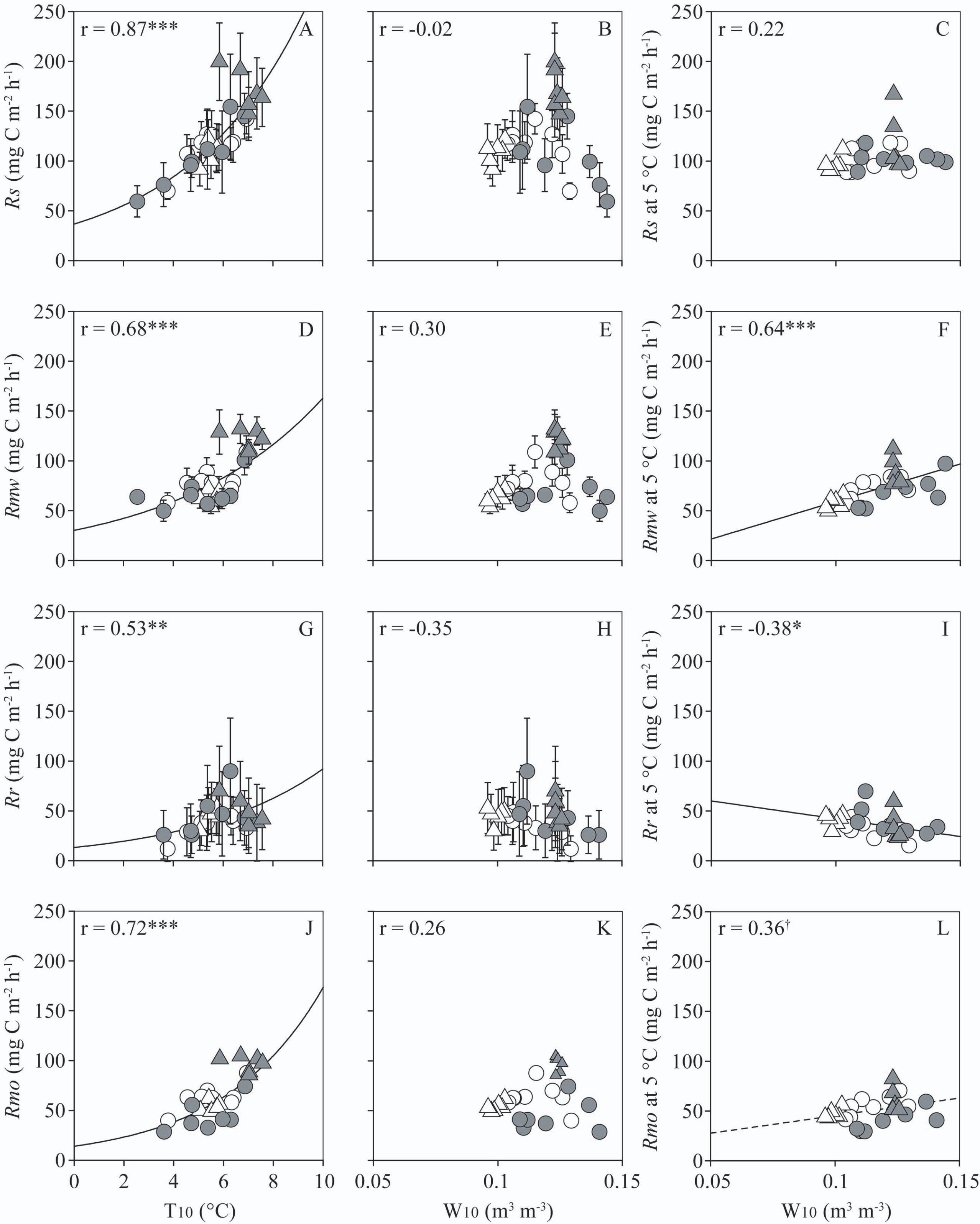

r = 0.87***
A
r = -0.02
B
r = 0.22
C
Rs (mg C m-2 h-1)
Rs at 5 °C (mg C m-2 h-1)
r = 0.68***
D
r = 0.30
E
r = 0.64***
F
Rmw (mg C m-2 h-1)
Rmw at 5 °C (mg C m-2 h-1)
r = 0.53**
G
r = -0.35
H
r = -0.38*
I
Rr (mg C m-2 h-1)
Rr at 5 °C (mg C m-2 h-1)
r = 0.72***
J
r = 0.26
K
r = 0.36†
L
Rmo (mg C m-2 h-1)
Rmo at 5 °C (mg C m-2 h-1)
T10 (°C)
W10 (m3 m-3)
W10 (m3 m-3)

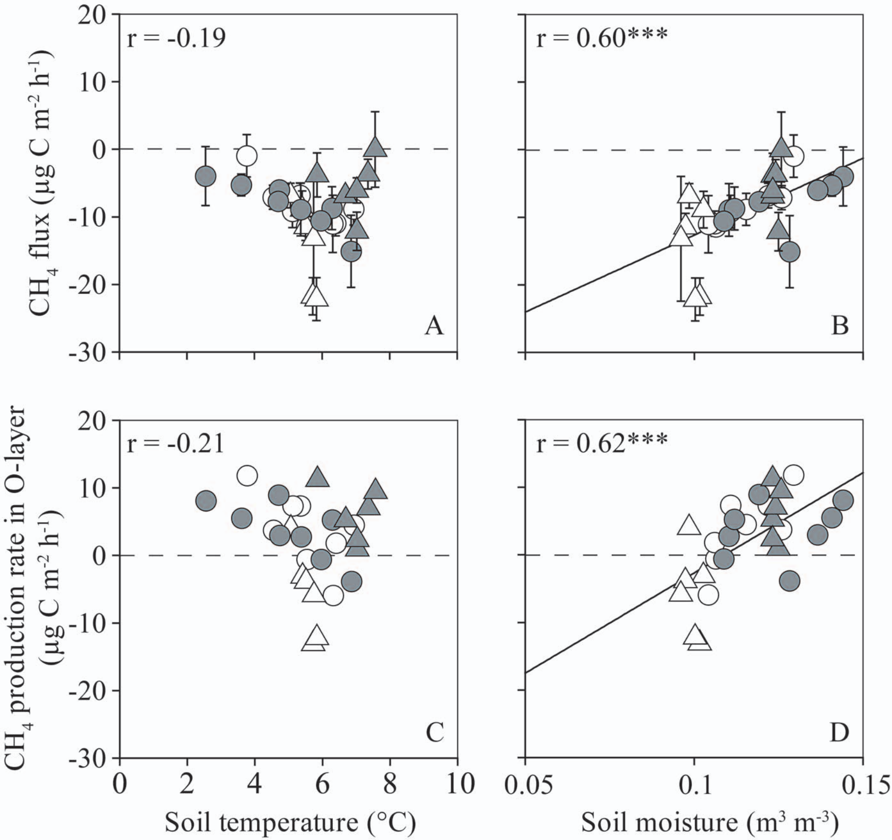

r = -0.19
r = 0.60***
r = -0.21
r = 0.62***
A
B
C
D
CH_4 flux (μg C m^{-2} h^{-1})
CH_4 production rate in O-layer (μg C m^{-2} h^{-1})
20
10
0
-10
-20
-30
0
2
4
6
8
10
0.05
0.1
0.15
Soil temperature (°C)
Soil moisture (m^3 m^{-3})

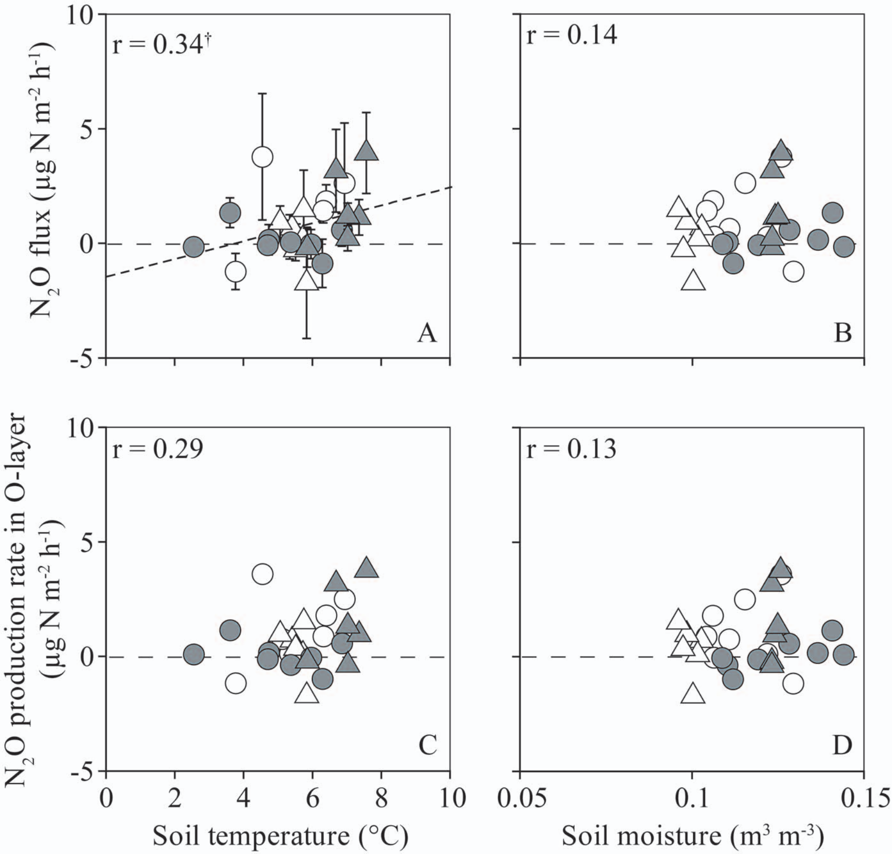

r = 0.34†
r = 0.14
r = 0.29
r = 0.13
A
B
C
D
N2O flux (µg N m-2 h-1)
N2O production rate in O-layer (µg N m-2 h-1)
Soil temperature (°C)
Soil moisture (m3 m-3)
10
5
0
-5
0
2
4
6
8
10
0.05
0.1
0.15

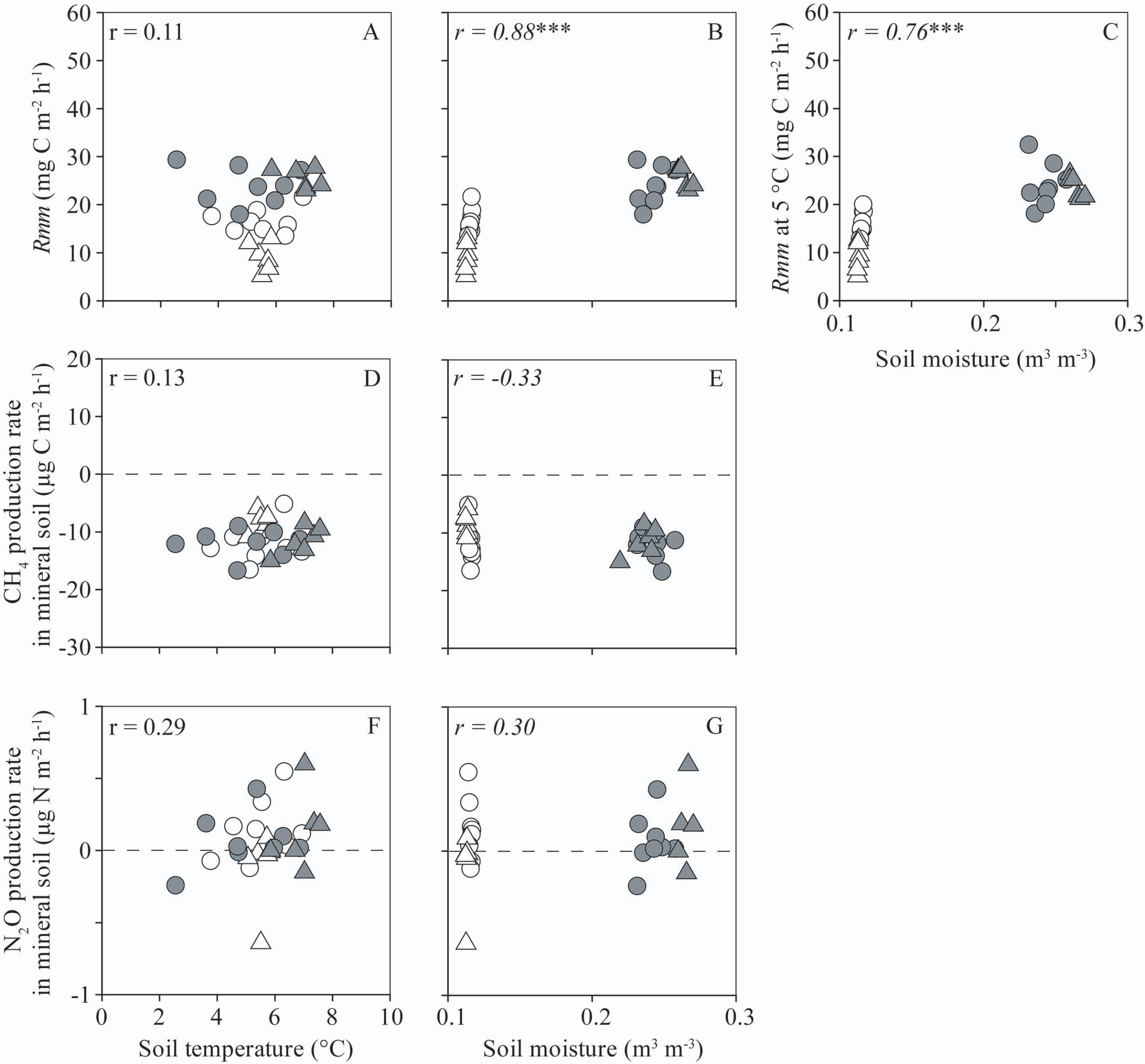

r = 0.11
A
r = 0.88***
B
r = 0.76***
C
Rmm (mg C m-2 h-1)
Rmm at 5 °C (mg C m-2 h-1)
Soil moisture (m3 m-3)
r = 0.13
D
r = -0.33
E
CH4 production rate in mineral soil (µg C m-2 h-1)
r = 0.29
F
r = 0.30
G
N2O production rate in mineral soil (µg N m-2 h-1)
Soil temperature (°C)
Soil moisture (m3 m-3)

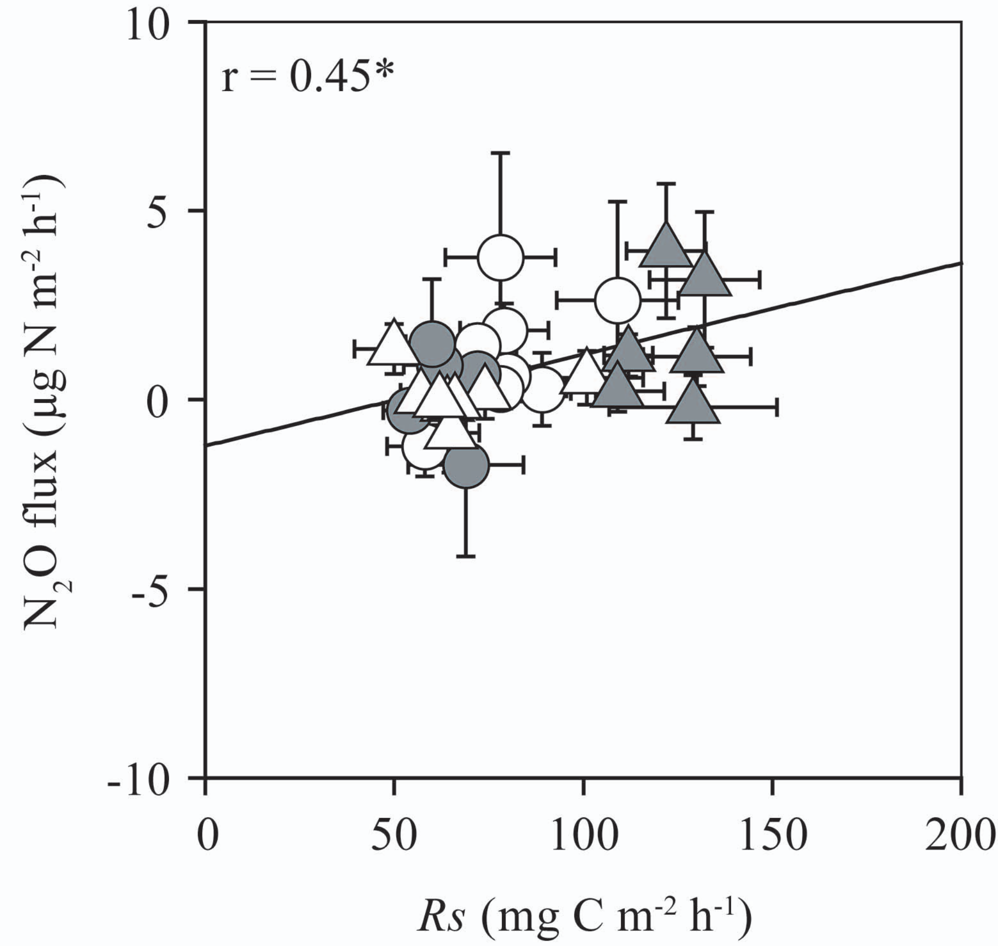
r = 0.45*
N_2O flux (μg N m^{-2} h^{-1})
10
5
0
-5
-10
0
50
100
150
200
Rs (mg C m^{-2} h^{-1})